Photodemethylation of methylmercury in Eastern Canadian Arctic thaw pond and lake ecosystems

*Catherine Girard[1], Maxime Leclerc[2], Marc Amyot[1,2]**

AUTHOR ADDRESS

1. Centre d'études nordiques (CEN), Département de sciences biologiques, Université de Montréal, 90 Vincent-d'Indy, Montréal, QC, Canada

2. Groupe de recherche interuniversitaire en limnologie et en environnement aquatique (GRIL), Département de sciences biologiques, Université de Montréal, 90 Vincent-d'Indy, Montréal, QC, Canada

KEYWORDS

Photodemethylation, methylmercury, thaw ponds, Arctic, organic matter, climate change, biogeochemistry

ABSTRACT

Permafrost thaw ponds of the warming Eastern Canadian Arctic are major landscape constituents and often display high levels of methylmercury (MeHg). We examined photodegradation potentials in high-dissolved organic matter (*DOC*) thaw ponds on Bylot Island (BYL) and a low-*DOC* oligotrophic lake on Cornwallis Island (Char Lake). In BYL, the ambient MeHg photodemethylation (PD) rate over 48 h of solar exposure was 6.1×10^{-3} m^2 E^{-1}, and the rate in MeHg amended samples was 9.3×10^{-3} m^2 E^{-1}. In contrast, in low-*DOC* Char Lake, PD was only observed in the first 12 hours, which suggests that PD may not be an important loss process in polar desert lakes. Thioglycolic acid addition slowed PD, while glutathione and chlorides did not impact northern PD rates. During an ecosystem-wide experiment conducted in a covered BYL pond, there was neither net MeHg increase in the dark nor loss attributable to PD following re-exposure to sunlight. We propose that high-*DOC* Arctic thaw ponds are more prone to MeHg PD than nearby oligotrophic lakes, likely through photoproduction of reactive species rather than via thiol complexation. However, at the ecosystem level, these ponds, which are widespread through the Arctic, remain likely sources of MeHg for neighbouring systems.

INTRODUCTION

Mercury (Hg) contamination is a major environmental issue in the Canadian Arctic, which is considered to be a sink for volatile anthropogenic Hg produced at lower latitudes.[1,2] After deposition in the Arctic environment, Hg can be methylated into methylmercury (MeHg) by certain iron or sulphate-reducing bacteria and methanogens in anoxic environments.[3–6] This dangerous neurotoxin then accumulates in aquatic ecosystems of Arctic Canada.[7,8] The Arctic's changing climate may also increase the risk posed by MeHg by accelerating permafrost thawing, contributing to a larger release of historically stored inorganic Hg[2,9–11] and possibly increasing its microbial methylation rates.[9,10,12] MeHg can represent a potential risk to northern communities by bioaccumulating and biomagnifying in foodwebs, eventually contaminating organisms that are part of the traditional diets of local human populations.[13]

Climate warming in the Arctic is currently promoting the formation of thermokarst thaw ponds. These ponds now represent the most abundant type of aquatic systems at Arctic and Subarctic latitudes.[14] In the Eastern Canadian Arctic, they are characterized by very high MeHg levels that are in some instances orders of magnitude higher than neighbouring oligotrophic lakes.[15] These ponds could constitute a source of MeHg for nearby lakes, streams and coastal waters and therefore contribute to the contamination of traditional food.

Photodemethylation (PD) of MeHg could reduce the risk posed by these high levels of MeHg in thaw ponds and has been documented in other polar ecosystems.[7,16–18] Both field and laboratory studies have found PD to be highly dependent on UV radiation.[19–26] A study conducted in an Alaskan lake found that PD does not appear to be driven by the direct photolysis of MeHg: an indirect pathway involving naturally occurring chemical actors seemed to be responsible for the demethylation process.[27] In oxygenated freshwater, MeHg is usually bound to organic matter[28]

which is likely involved in PD.[29,30] Sulphur-rich functional groups of organic matter (thiols), to which MeHg preferentially binds, are suspected of promoting PD.[18,31] Organic matter may also be involved in PD through its photo-mediated production of reactive oxygen species (*ROS*),[18,32] or via intramolecular electron transfer.[30] Source and quality of organic matter have been found to significantly influence PD rates.[20,29,33] Organic matter can also reduce light penetration in aquatic ecosystems.[34] Chloride complexation however has been reported to limit PD, explaining the discrepancy in rates observed between marine and freshwater ecosystems.[18,20]

This study aimed to (1) establish via field-based experiments if PD occurs in permafrost thaw ponds of the Eastern Canadian Arctic and if PD rates are higher than in oligotrophic lakes. We chose sites similar to each other in terms of water chemistry, except for their contrasting levels of organic matter, which could induce variation in PD potential. (2) Using field and laboratory experiments, we also sought to identify the chemical actors involved in PD, namely thiols found either free in the water column or as functional groups of dissolved organic matter, and chlorides. (3) Finally, we conducted an ecosystem-wide experiment to assess the potential impacts of PD on MeHg levels in thaw ponds.

MATERIALS AND METHODS

Field area and sampling sites

Sampling was performed on Bylot and Cornwallis Islands in the Canadian Arctic Archipelago from June to August 2010 and 2011 during the Arctic summer in 24-hour daylight.

Experiments in the polar oasis of Bylot Island (73°9'23.4" N**;** 79°58'19.38" W) were conducted in permafrost thaw ponds of the Qarlikturvik glacial valley. These ponds (henceforth referred to

as BYL sites) are small unstratified aquatic ecosystems formed from degradation of ice wedges and thawing of permafrost[14] and contain high levels of dissolved organic carbon[35] (*DOC*: 6.20-9.60 mg L^{-1}) and of Hg (Hg: 1.14-30.20 ng L^{-1}; MeHg: 0.06-18.19 ng L^{-1}).[15]

Char Lake was sampled on Cornwallis Island (74°41'11.20" N; 94°54'33.81" W). Due to its low plant productivity, Cornwallis is considered a polar desert,[36] where lakes are highly oligotrophic (*DOC*: 0.94 mg L^{-1}) and typically have low levels of Hg (Hg: 0.22-0.80 ng L^{-1}; MeHg: 0.01-0.07 ng L^{-1}).

Map of sites, surface water chemistry, Hg measurements and light parameters of individual sampled sites are presented in Supporting Information (SI, Figure S1 and Table S1).

Sampling methods

Water was sampled using an acid-washed peristaltic pump and filtered with a high-capacity 0.45 μm filtration cartridge (Pall Life Sciences). Dissolved organic carbon (*DOC*) samples were stored in glass amber bottles that were burnt at 550 °C for 2 hours prior to sampling. High-density polyethylene bottles were used for thiol, cation and anion samples. Thiols and cations were collected in acid-washed bottles, and anion samples in MilliQ-rinsed bottles (ultra-pure 18.2 MΩ cm water, EMD Millipore). PD experiments were conducted with acid-washed Teflon FEP bottles and experimental solutions were kept in amber glass bottles with polytetrafluoroethylene-lined polypropylene caps. Hg and MeHg samples were preserved with OmniTrace Ultra HCl (OmniTrace Ultra, VWR) (final concentration of 0.4%) while following the 'clean hands, dirty hands' protocol.[37] Pump and bottle washing procedures are detailed in SI (Supplementary Methods).

Experimental design

PD field experiments were conducted in natural sunlight. Water was collected in clear Teflon bottles with no headspace. At every time-point during incubations, a triplicate of every treatment series (duplicates for some dark controls) was removed from the incubation set-up and preserved with ultrapure HCl to a 0.4% final concentration. Detailed methods are described in SI.

Experiments measuring natural rates in BYL24 and Char Lake included three treatments: dark, exposure to full solar spectrum and exposure to visible light only, using UV filters (Lee 226, Lee Filters).

Mechanistic experiments studying the effect of chemical actors on PD over 48 h were conducted in BYL22 and Char Lake, with water amended to 5.0 ng L^{-1} (± 0.4%) of MeHg (Certified standard solution, Alfa Aesar) (Details on certified standards are provided in Supplementary Methods). Treatments included thiols (10.0 nM *GSH*, 10.0 nM thioglycolic acid (*TA*); >98%, MP Biomedical and Sigma-Aldrich) and chlorides (0.6 M NaCl; Certified ACS, Fisher Scientific). Thiol levels were chosen to significantly increase ambient concentrations, while staying in the range of concentrations measured in North American freshwaters.[38–42] Chloride concentration was selected to represent marine conditions, to investigate the wide difference in PD reported for fresh and saltwater,[18,20] and to assess the potential role of marine intrusion into coastal Arctic ponds.[43] This experiment was repeated in the laboratory with BYL22 and MilliQ water using a solar simulator (Suntest CPS+, Atlas Material Testing Technology). Additional experiments were conducted on waters from a temperate Canadian Shield lake[44] (45°59'35" N**;** 74°00'28" W), with amendments of up to 1000 nM *GSH*. To insure comparability

between field and laboratory experiments, the solar simulator was programmed to deliver a total dose (E m^{-2}) equal to that received during field incubations (see SI for detailed explanations).

Finally, to assess the potential impact of PD on the MeHg budget of a small aquatic ecosystem, we sampled BYL22 every 6 h (surface and 30 cm depth) over a 14-day period for total Hg and MeHg and water chemistry parameters. During days 4-8, the pond was covered with a clean opaque plastic tarpaulin anchored into the surrounding permafrost. Pump and sensor tubing were permanently installed at the desired depths to limit disturbances and light penetration associated with sampling. Detailed methods including ambient light and temperature conditions are described in SI.

MeHg photodemethylation rates

PD rates (k_{PD}) were obtained by modeling the evolution of MeHg concentrations against cumulative *PAR* with apparent first-order reaction kinetics:

$$\ln([\mathrm{MeHg}]_t) = \ln([\mathrm{MeHg}]_0) - k_{PD} PAR_t \quad (1)$$

where $(\mathrm{MeHg})_0$ is the initial MeHg concentration (ng L^{-1}), $(\mathrm{MeHg})_t$ is the MeHg concentration (ng L^{-1}) at time t, PAR_t is the cumulative *PAR* (E m^{-2}) received at time t, and k_{PD} is the PD apparent rate constant (m^2 E^{-1}).

MeHg concentrations also exhibited apparent first-order reaction kinetics as a function of incubation time. However, *PAR* was a better predictor than exposure time, and allowed for comparisons between sites and years. When *PAR* measurements were not available, k_{PD} values were calculated over incubation time.

As Teflon attenuates a small portion of solar radiation, all rates were adjusted to correct the attenuation of light by the bottles' material.[45]

Analytical methods

Hg concentrations were quantified using cold-vapour fluorescence spectrometry (CVAFS) (Tekran 2600, Tekran Instruments Corporation), following U.S. EPA method 1631 (detection limit of 0.04 ng L^{-1}). MeHg was measured by gas chromatography and CVAFS (Tekran 2500 and 2700, Tekran Instruments Corporation), according to U.S. EPA method 1630 (detection limits of 0.02 ng L^{-1} and 0.0004 ng L^{-1}, respectively). Detection limits were defined as three times the standard deviation calculated on 10 ultrapure MilliQ blanks. A field detection limit was also calculated as three times the standard deviation of dark controls. Detailed analytical methods are described in Perron et al.[44] Hg analyses met the criteria of the Canadian Association for Laboratory Accreditation (CALA) inter-calibration. *DOC*, ion and thiol analyses are described in SI. Speciation calculations were conducted with the Windermere Humic Aqueous Model (WHAM7 - http://www.ceh.ac.uk/services/windermere-humic-aqueous-model-wham).[46]

Statistical analyses

Statistical analyses ($\alpha = 0.05$) were done with R software.[47] Linear regressions were used to model changes in MeHg concentrations and to calculate k_{PD}. Only significant slopes were considered. Data points presented are from duplicate (dark controls) or triplicate bottles (treatment series), while error bars show standard deviation. Slopes were compared using

analysis of covariance (*ANCOVA*) with Bonferroni's correction where multiple comparisons were made. Analyses of variance (*ANOVA*) paired with Tukey's test and Kruskal-Wallis non-parametric analyses were used to compare conditions before and after manipulations in the covered pond experiment. Means were compared with Student's t-test.

RESULTS & DISCUSSION

Photodemethylation in BYL ponds and Char Lake

In all field experiments of Arctic waters, filtered samples incubated in sunlight showed decreasing MeHg concentrations, while MeHg levels in samples kept in the dark remained stable. We therefore conclude that MeHg losses observed in our incubation experiments are attributable to abiotic PD (Figures 1, 2 and 3).

In BYL24, PD only occurred in the presence of *UVs* (k_{PD} of $6.1 \pm 0.7 \times 10^{-3}$ m^2 E^{-1}) (Figure 1). This supports findings of other authors, identifying *UVs* as the main waveband responsible for PD.[8,17,19,20,26] Field experiments lasting 48 hours conducted in BYL22 with 5.0 ng L^{-1} MeHg amendments yielded a k_{PD} of $9.3 \pm 1.5 \times 10^{-3}$ m^2 E^{-1} (Figure 2A). This resulted in the loss of 56.6% of initial MeHg (Figure 2A).

During the 9-day incubation experiment in low-*DOC* Char Lake, ambient MeHg levels were very low, and sometimes below the field detection limit (SI, Figure S2): no k_{PD} could therefore be calculated. In spiked Char Lake water (5.0 ng L^{-1} MeHg), no significant k_{PD} was found after 48 hours (p-value > 0.05) (Figure 2B). However, final MeHg concentrations differed from the initial MeHg value and from the dark control (p-value < 0.05), and 16.4% of initial MeHg was lost over

the course of the 9-day incubation: this is explained by the significant slope found in the first 12 hours of the experiment, (k_{PD} of 19.3 ± 5.9 × 10^{-3} m^2 E^{-1}) (Figure 2B inset). This underscores the importance of assessing early photo-mediated reactions in long-term incubations.

MeHg levels at both sites differed by one order of magnitude (SI, Table S1). Since PD has been found to be independent of MeHg concentrations,[19,20] differences in k_{PD} may be due to another contrasting characteristic of the BYL ponds and Char Lake, such as their *DOC* concentrations (respectively 6.20 to 9.60 and 0.94 mg L^{-1}) (SI, Table S1). We investigated if this contrast in *DOC* levels resulted in differences in MeHg speciation, using the thermodynamic model WHAM.[46] MeHg speciation was similar in both lakes with 75% of MeHg bound to fulvic acids in Char Lake, compared to 89% in BYL22. The potential effect of *DOC* on PD is therefore likely not achieved via differences in MeHg-*DOC* complexation in these two systems, but rather by other roles of *DOC* (e.g. generation of *ROS*, see below). It is also possible that differences in *DOC* quality may modify its complexation properties with an impact on PD,[31,33] as has been shown in the photo-production of another Hg species, dissolved gaseous Hg.[48] Information on changes in *DOC* fluorescence can be used as a proxy for *ROS* production,[48] and would provide valuable insight into *DOC*-mediated PD in these sites.

Char Lake can be compared to another Arctic lake (Toolik Lake), which has a similar near-neutral pH and comparable MeHg concentrations in surface waters (respectively 0.02 ng L^{-1} and 0.05 ng L^{-1})[7] (SI, Table S1 and S2). However, *DOC* concentrations in Char Lake (0.94 mg L^{-1}) are lower than those measured in Toolik Lake (4.44 mg L^{-1}).[7] While no PD was measured in unspiked waters of Char Lake over 9 days, it has been observed in Toolik Lake over 6 day-incubations (2.6 × 10^{-3} m^2 E^{-1}).[7] This further points to organic matter as an important driver of

PD, as has been reported by other authors,[18,20,29] and suggests that *DOC* could explain the discrepancy between PD rates in Char Lake and the BYL ponds.

Overall, these results clearly indicate that thermokarst thaw ponds are sites of PD whereas no significant PD could be measured in unspiked waters of the oligotrophic Char Lake. To our knowledge, the results from the polar lake is the first instance of a freshwater system where PD is so limited, therefore providing boundaries to the presumed universal importance of this process.

Thiols and photodemethylation

Thiols can be found in natural waters in their low molecular weight (*LMW*) form or as a functional group of organic matter,[49] and have previously been identified as promoters of PD in simulated waters.[18] In their *LMW* form, we measured at the study sites *GSH* and *TA* concentrations of 0.2 ± 0.1 nM and of 5.1 ± 1.6 nM, respectively. As functional groups of organic matter (assuming 7.3 x 10^{-5} moles reduced–S per gram of C),[50] thiols ranged from 70 nM (Char Lake) to 450 nM (BYL22), largely exceeding MeHg concentrations, as they do in most pristine environments.[49] To determine if the action of *DOC* in mediating PD was limited by the concentration of thiol binding sites, incubation experiments were conducted in the field and in a solar simulator with thiol additions in the environmentally-relevant range of 10 to 1000 nM.

In an experiment conducted in natural sunlight in spiked BYL22 water (5.0 ng L^{-1} MeHg), 10 nM *TA* amendments (which doubled natural dissolved *TA* concentrations) slowed k_{PD} by 33.3%, from 9.3 ± 1.5 × 10^{-3} m^2 E^{-1} in the control series to 6.2 ± 1.0 × 10^{-3} m^2 E^{-1} (Figure 3A) (p-value < 0.05).

In field experiments in Char Lake, no significant relationship was observed between time and MeHg concentration (p-value > 0.05), and 10 nM *GSH* amendments (increasing natural dissolved *GSH* concentrations by 50-fold) did not induce PD (Figure 3B). However, when considering only the first 12 hours of the experiment (Figure 3B Inset), the control and *GSH* series both yielded significant k_{PD} (respectively 19.3 ± 5.9 × 10^{-3} m^2 E^{-1} and 19.3 ± 4.0 m^2 E^{-1}), that did not however differ from one another (p-value > 0.01).

In incubations in a solar simulator with BYL22 water, *GSH* amendments had no significant effect on PD when compared to control rates (*GSH* k_{PD}: 11.0 ± 0.8 × 10^{-3} m^2 E^{-1}; control k_{PD}: 11.3 ± 2.4 × 10^{-3} m^2 E^{-1}) (p-value > 0.01 with Bonferroni's correction) (Figure 3C). Likewise, *GSH* had no impact in spiked MilliQ water in simulated light conditions (Figure 3D). Dark controls remained stable during incubations (Figure 3D). Both in BYL22 and Char Lake, thiols therefore had diverging effects on PD, with *TA* reducing k_{PD} and *GSH* having no impact.

Supplementary PD experiments conducted in water from a temperate lake showed that adding 10 nM *GSH* to this natural matrix lead to a k_{PD} similar to that of the control series, confirming results from BYL22 in simulated light (SI, Figure S5). Increasing *GSH* concentrations to 100 nM and 1000 nM increasingly slowed PD until it did not differ from dark controls (SI, Figure S5). Previous work has found that PD of MeHg bound to non-aromatic thiols (such as *GSH*) is slower than that of MeHg bound to aromatic thiols or *DOC*.[33] Furthermore, in a study using simulated freshwater, PD was fastest when MeHg was bound to *DOC*, slowest for MeHg-thiol complexes only, and intermediate when both *DOC* and thiols were present.[51] These studies suggested that PD is possible through an intramolecular mechanism, where light is absorbed by *DOC* and energy is then transferred to break the Hg-C bond:[33,51] Adding thiols could thus remove some or all of the MeHg bound to *DOC*, preventing this intra-*DOC* process from occurring and thus

slowing PD.[51] This could explain why increasing concentrations of *GSH* slowed and eventually halted PD in temperate waters (SI, Figure S5).

It is also important to consider *GSH* degradation during incubation experiments. In temperate lake water, *GSH* was also simultaneously degraded during exposure to light (approximately 30% after 5 hours) (SI, Figure S6), as has been previously reported.[52] *GSH* degradation can depend on the matrix and on other ions present. Indeed, some metals such as copper may affect the oxidation states of *GSH* and potentially lead to other degradation products.[18,52] In BYL ponds, *GSH* may have been partly degraded before being able to fully intervene in PD.

Overall, thiol addition did not promote PD in different natural waters in these experiments. These results are in general agreement with the study of Tai et al. performed in the Florida Everglades.[30]

Photodemethylation mediated by ROS radicals

Although they have highly contrasting *DOC* levels, WHAM simulations showed that Char Lake and BYL22 have similar *DOC* speciation, suggesting that MeHg-*DOC* complexation is not the cause of the difference observed in k_{PDs}. Furthermore, in both sites, thiol concentrations largely exceed that of MeHg, and while thiols complex MeHg efficiently and are likely implicated in photochemical reactions of Hg, MeHg-thiol complexation does not explain the difference in PD potential seen here. As *DOC* is consistently found to have an important role in mediating PD,[18,20,29] and is the main difference between Char and other Arctic lakes and ponds where PD was observed (Toolik Lake, BYL ponds), we propose that the discrepancy in observed k_{PDs} may be due to other roles of organic matter, such as the photoproduction of *ROS* radicals in

the photic zone.[53,54] *ROS* are suspected of mediating PD, as quenchers for these molecules have been found to limit PD in sea water,[21] in simulated waters[18,22] and in an Arctic oligotrophic lake.[27]

In a study conducted on lakes of a wide array of limnological characteristics, Char Lake was found to have the lowest formation rate of hydrogen peroxide (6.95 mg m^{-2} d^{-1}), a *DOC*-produced *ROS* that closely correlated to *DOC* concentrations.[55] If Char Lake is equally poor in other *ROS*, it may be a non-conducive environment for PD. Early PD (Figure 2B inset) may have occurred before the rapid depletion of naturally-occuring *ROS* in experimental bottles.

We hypothesize that PD in Char Lake may be partially controlled by *ROS* and organic radicals produced during *DOC* photolysis.[26] This supports observations by other authors that *DOC* may act as a catalyzer for PD, more than simply a light attenuator or complexation agent,[20] and the role of *ROS* should be further investigated. As no experiments in the present study directly measured the role of *ROS* on PD, we can only speculate on their potential role. Further field-based experiments are necessary to better understand the role of photo-produced *ROS* from *DOC* in natural waters.

Relationship between DOC and k_{PD}

A comparison of Arctic PD studies shows that up until a threshold, *DOC* exhibits a positive (yet not significant) relation with k_{PD} (Figure 4A), with polar desert Char Lake representing the lower limit of this relationship. When non-Arctic studies are included, no significant relationship is found, but the same general trend is observed (Figure 4B). There may be a breakpoint after which *DOC* inhibits PD. We propose that at lower *DOC* levels, PD is limited by *ROS* concentrations, while at *DOC* levels above this threshold, complexation or UV attenuation may

be more important. Other studies on Hg and *DOC* in aquatic ecosystems have found comparable thresholds for Hg bioaccumulation/bioavailability[56,57] and for production of dissolved gaseous Hg.[48] A similar relationship may exist between *DOC* and PD. This observation is based on few studies and may be due to differences in experimental designs, and requires further investigation. More aquatic ecosystems should be sampled across a wider range of *DOC* values to assess this potential breaking point.

The low PD rates recorded in low-*DOC* Char Lake question the expectation of PD being the main degradation pathway for MeHg in low-DOC oligotrophic ecosystems with good light penetration.[7,19,27] Oligotrophic Arctic lakes like Char Lake are typically characterized by low *DOC* levels,[58] and permafrost-influenced regions hold the greatest number of lakes in the northern hemisphere.[59] If climate change alters *DOC* input into these ecosystems, this could change PD potential and MeHg mass balances in Arctic aquatic ecosystems.

Photodemethylation mediated by chlorine

Previous authors have observed a negative relationship between PD rate and Cl concentrations,[20,24] and the complexation of MeHg to chloride ions has been used to explain lower k_{PD} values observed in the marine environment.[18,20,60,61] We therefore tested the effect of chlorides in spiked (5.0 ng L^{-1} MeHg) BYL22 water, which yielded a k_{PD} of $6.7 \pm 0.6 \times 10^{-3}$ m^2 E^{-1} (p-value < 0.05), which did not differ significantly from the control rate (p-value > 0.008 with Bonferroni's correction) (Figure 3A). In Char Lake, no PD was observed in control and Cl treatment series (Figure 3B).

At high Cl concentrations, the main species of MeHg is thought to be CH_3HgCl, with the strength of the Hg-Cl bond preventing MeHg decomposition.[24] Indeed, in our field experiments, adding 0.6 M of NaCl led to a shift in MeHg speciation from the *DOC*-bound pool to the CH_3HgCl pool (with the *DOC*-bound pool decreasing from 89 to 8% of the total in BYL22 and 75% to 29% in Char, according to calculations done with WHAM7). Therefore, adding Cl altered MeHg complexation, but did not slow PD. Chlorides have also been reported to accelerate PD by producing chlorine radicals capable of attacking the Hg-C bond.[22] However, other authors have suggested that increasing salinity may also quench *ROS*, slowing PD.[20] These competing processes involving chlorides may explain why adding Cl did not impact PD in these experiments.

Ecosystem-scale observations of photodemethylation

To assess the impact of PD at the ecosystem level, BYL22 was monitored during 14 days, with a plastic tarpaulin covering the pond during Days 4-8. This blocked 98.7% of radiation from 290-895 nm, and 100% of radiation in the UV spectrum (400 nm ≤ λ) (SI, Figure S7). On Day 7, gusts of wind ripped off the cover, exposing the pond for approximately three hours. Light exposure was minimal, as this occurred shortly after midnight, when the sun is at its lowest. This is nonetheless reflected in measurements taken at 6:00 a.m. on Day 7 (see dotted line, Figure 5).

Based on the rate previously measured in BYL22, PD was expected to remove up to 85% of MeHg at the surface during the 5 days following re-exposure to sunlight (Days 9-13) (See SI). However, MeHg concentrations did not decrease from Days 9-13: indeed, MeHg levels were higher on Day 13 than on Day 9 both in surface waters (Day 9: 0.14 ± 0.01 ng L-1; Day 13: 0.23

± 0.02 ng L^{-1}) and at 30 cm (Day 9: 0.13 ± 0.03 ng L^{-1}; Day 13: 0.24 ± 0.03 ng L^{-1}) (*p*-value < 0.05). Free *LMW* thiol concentrations on the other hand decreased sharply following re-exposure of the pond to sunlight (from 16.56 to 6.85 nM over 18 h), suggesting a massive thiol photodegradation event (Figure 5C), with a slight lag potentially due to the persistence of these molecules in freshwater that ranges from hours to days.[52] This thiol degradation could have been caused by *ROS* produced from irradiated organic matter,[52] which could have contributed to PD. However, no decrease of MeHg was observed after surface waters were re-exposed. Over the course of the experiment, MeHg levels were higher after re-exposure to sunlight than when the experiment began, both at the surface (mean before cover: 0.16 ± 0.03 ng L^{-1}; mean after re-exposure: 0.22 ± 0.06 ng L^{-1}) and at 30 cm (0.15 ± 0.04 ng L^{-1}; 0.21 ± 0.04 ng L^{-1}) (*p*-value < 0.05; Figure 5A).

While temperatures remained stable during the covered period (9.33 ± 1.32 °C at the surface and 8.43 ± 1.54 °C at 30 cm) (Figure 5D), a chemical stratification was induced, which is exceptional for this type of shallow, normally well-mixed site (Figure 5E-G). Notably, near-hypoxic conditions developed at the water-sediment interface less than 24 hours into the dark treatment (3.68 ± 2.64 mg L^{-1}), while surface levels remained stable (9.07 ± 1.03 mg L^{-1}) (Figure 5E). This may have improved conditions for microbial methylation of inorganic Hg, leading to increased MeHg production during the covered period. Lack of mixing and the flocky nature of the sediments would likely have sequestered newly produced MeHg for some time, which became detectable only once it had diffused to 30 cm below the surface after the cover was removed (Figure 5A). The increase in MeHg following re-exposure of surface waters to sunlight may also be attributable to phototrophic blooms, which can create environments that can

facilitate methylation of Hg.[62] Therefore, if PD occurred, it may have been obscured by *in situ* MeHg production, resulting in a 43% net increase in MeHg concentrations (Figure 5A).

PD is frequently cited as a major degradation pathway of MeHg[7,8,19,20,63] and is often included in mass Hg budgets for aquatic ecosystems, where rates are extrapolated from bottle experiments to whole-lake levels. Following the observation of PD in BYL22 via bottle incubations, covering the entire pond with a tarpaulin was expected to have a significant impact on MeHg concentrations. Indeed, MeHg levels were expected to rise during the 4-day covered period, and to decrease following re-exposure to sunlight due to PD. However, no net decreases of MeHg were observed in the manipulated pond (Figure 5A).

In lakes, substantial PD can occur in the photic zone before UV attenuation, making it a major pathway for MeHg degradation.[7,63] In contrast, in very shallow aquatic ecosystems such as the BYL ponds, UV radiation likely penetrates at least partially to the bottom of the short water column, allowing for interactions with bottom processes such as abiotic[64] and microbial methylation and demethylation.[65] These overlapping sediment and photo-reactive processes could potentially blur the signal for PD, explaining why no PD was observed in this covered pond experiment. This interaction is of particular importance in the Arctic, where shallow thermokarst thaw ponds are the most abundant aquatic ecosystem.[14] Studies on isotopic fractionation could help in better untangling sediment and surface processes, as they have previously been used to investigate PD[31] and Hg photoreduction.[66]

While the design of this experiment could be improved upon, it constitutes a novel approach to study PD in shallow systems such as thermokarst thaw ponds, and emphasizes the importance of competing processes in the ecosystem. Alongside Lehnherr et al.'s extensive study of ponds in the Lake Hazen area (Nunavut),[8] this represents one of the first studies on Hg PD in a northern

system where surface and bottom processes are coupled. While bottle experiments provide essential insight into mechanistic reactions involved in PD, caution must thus be used when applying incubation rates to mass balance budgets across a range of aquatic ecosystems. The bottle effect may mask other reactions involved in the aquatic cycle of Hg, leading to an overestimation of the overall net impact of PD.

These results are important since they suggest that thermokarst thaw ponds recently shown to display high MeHg levels[15] are unlikely to see their MeHg pool decrease significantly via PD. It is likely that, because of the shallow nature of these ponds, processes occurring in the surface waters are directly affected and in competition with processes occurring at the sediment/water interface. These ponds may therefore be sources of MeHg for other systems, including nearby streams, lakes and coastal areas in which native communities tend to fish. Results from Char Lake indicate that PD may not be a significant process in polar desert lakes, likely because of very low *DOC* levels.

FIGURES

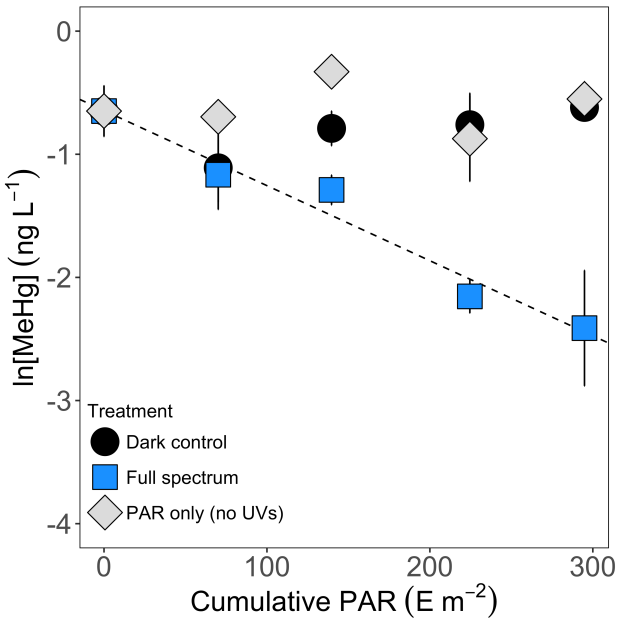

Figure 1. Natural logarithm of MeHg concentrations (ng L^{-1}) plotted against cumulative *PAR* (m^2 E^{-1}) during field experiments in BYL24. Filtered samples that were exposed to the full solar spectrum produced a k_{PD} of 6.1 ± 0.7 × 10^{-3} m^2 E^{-1} (p-value < 0.05, R^2 adjusted = 95.5%); dark controls and filtered samples covered by a UV filter yielded no significant relationship (not shown).

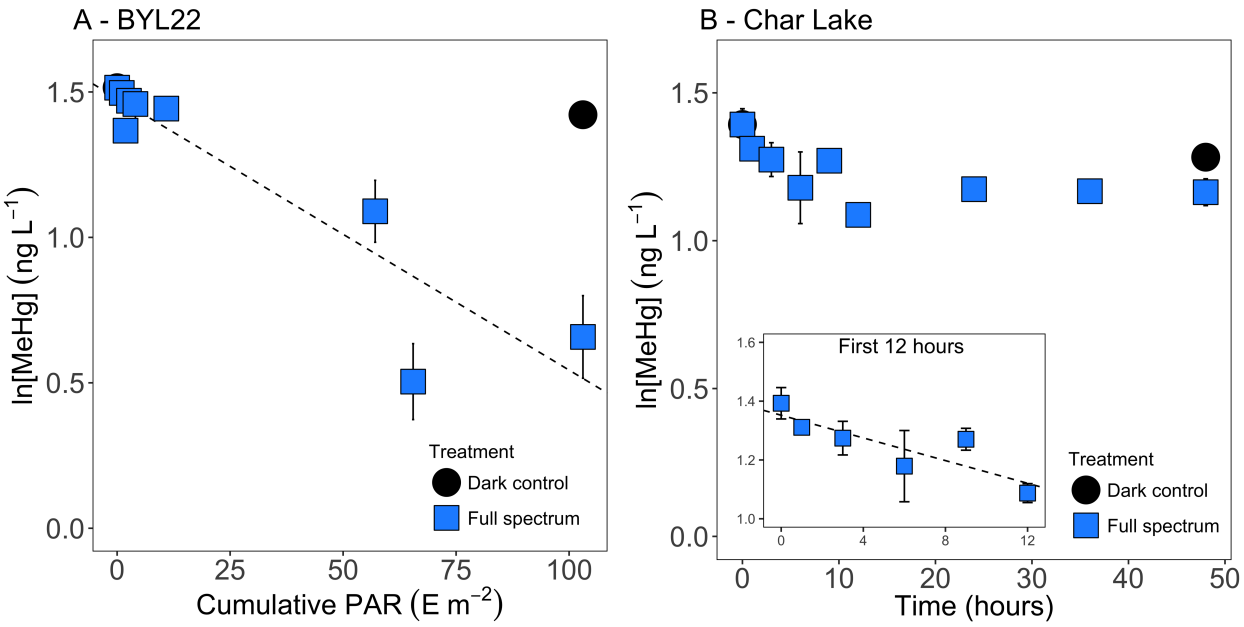

Figure 2. Natural logarithm of MeHg concentrations (ng L^{-1}) plotted against cumulative *PAR* (m^2 E^{-1}) during field experiments. **A.** In BYL22, MeHg amended samples that were exposed to the full solar spectrum produced a k_{PD} of 9.3 ± 1.5 × 10^{-3} m^2 E^{-1} (p-value < 0.05, R^2 adjusted = 82.0%). **B.** In Char Lake, no significant relationships were observed in any of the treatment series over 48 hours (regression p-values > 0.05). Inset: during the first 12 hours of incubation, samples exposed to the full solar spectrum yielded a k_{PD} of 19.3 ± 5.9 × 10^{-3} m^2 E^{-1} (p-value < 0.05, R^2 adjusted = 66.0%).

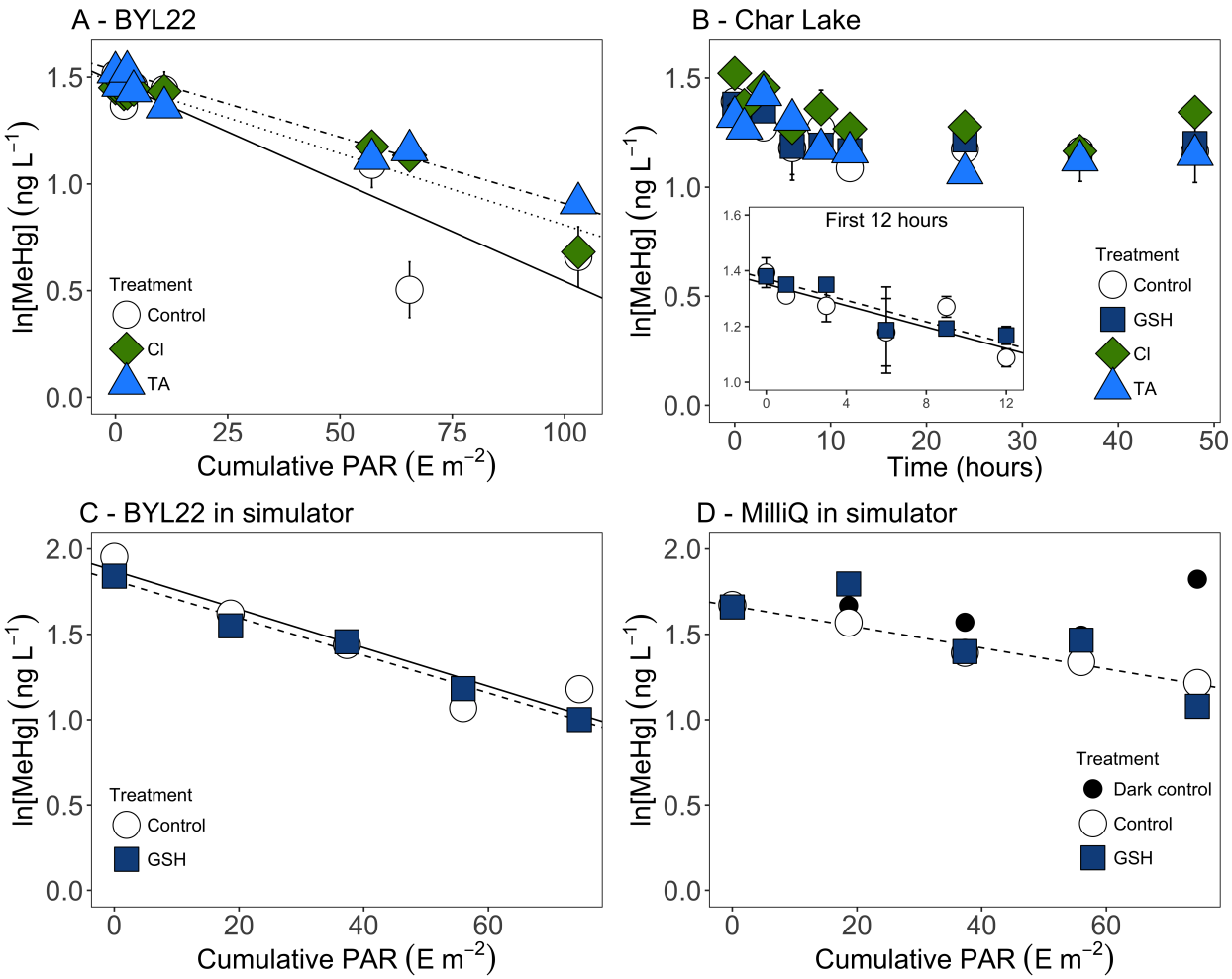

Figure 3. Natural logarithm of MeHg concentrations (ng L^{-1}) plotted against cumulative *PAR* (m^2 E^{-1}) received or incubation time (hours) in the field. **A.** In BYL22, the k_{PD} in spiked natural water was 9.3 ± 1.5 × 10^{-3} m^2 E^{-1} (p-value < 0.05, R^2 adjusted = 82.0%); in the Cl series, k_{PD} was 6.7 ± 0.6 × 10^{-3} m^2 E^{-1} (p-value < 0.05, R^2 adjusted = 93.5%); in the *TA* series, k_{PD} was 6.2 ± 1.0 × 10^{-3} m^2 E^{-1} (p-value < 0.05, R^2 adjusted = 82.1%). k_{PD} did not differ significantly from control rate (p-value > 0.01). **B.** In Char Lake, no significant relationships were observed in any of the treatment series over 48 hours (regression p-values > 0.05). Inset: first 12 hours of incubation, during which the control series yielded a k_{PD} of 19.3 ± 5.9 × 10^{-3} m^2 E^{-1} (p-value < 0.05, R^2 adjusted = 66.0%), while samples amended with *GSH* produced a k_{PD} of 19.3 ± 4.0 × 10^{-3} m^2 E^{-1} (p-value < 0.05, R^2

adjusted = 82.1%). No significant relationship was observed in the Cl and *TA* treatment series. **C.** In BYL22 water incubated in a solar simulator, the k_{PD} was $11.3 \pm 2.4 \times 10^{-3}$ m^2 E^{-1} (p-value < 0.05, R^2 adjusted = 84.0%); in the *GSH* series, k_{PD} was $11.0 \pm 0.8 \times 10^{-3}$ m^2 E^{-1} (p-value < 0.05, R^2 adjusted = 97.7%). *GSH* treatment did not differ from control rate (p-value > 0.05). **D.** In spiked MilliQ water incubated in a solar simulator, the k_{PD} was $6.1 \pm 0.5 \times 10^{-3}$ m^2 E^{-1} (p-value < 0.05, R^2 adjusted = 97.3%); and in the *GSH* series, no significant relationship was observed (not shown).

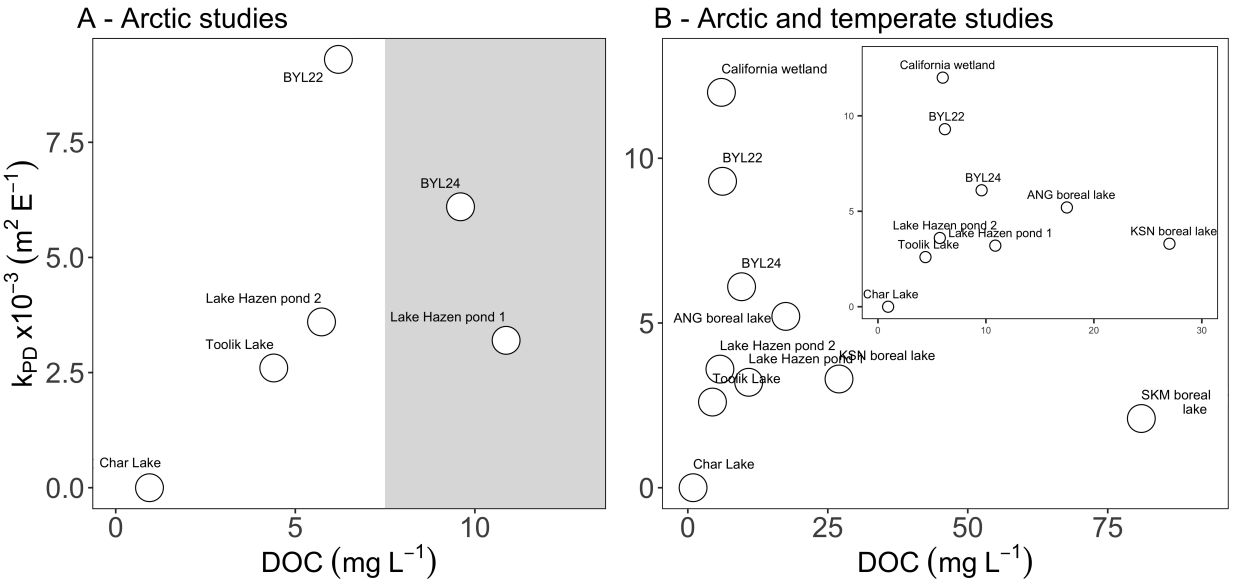

Figure 4. A. Relationship between k_{PD} (m^2 E^{-1}) and *DOC* (mg L^{-1}) from PD studies conducted in the Arctic only. Shaded area represents values above the potential threshold value. **B.** Relationship between k_{PD} (m^2 E^{-1}) and *DOC* (mg L^{-1}) from Arctic and temperate PD studies. Inset: *DOC* concentrations below 30 mg L^{-1}).

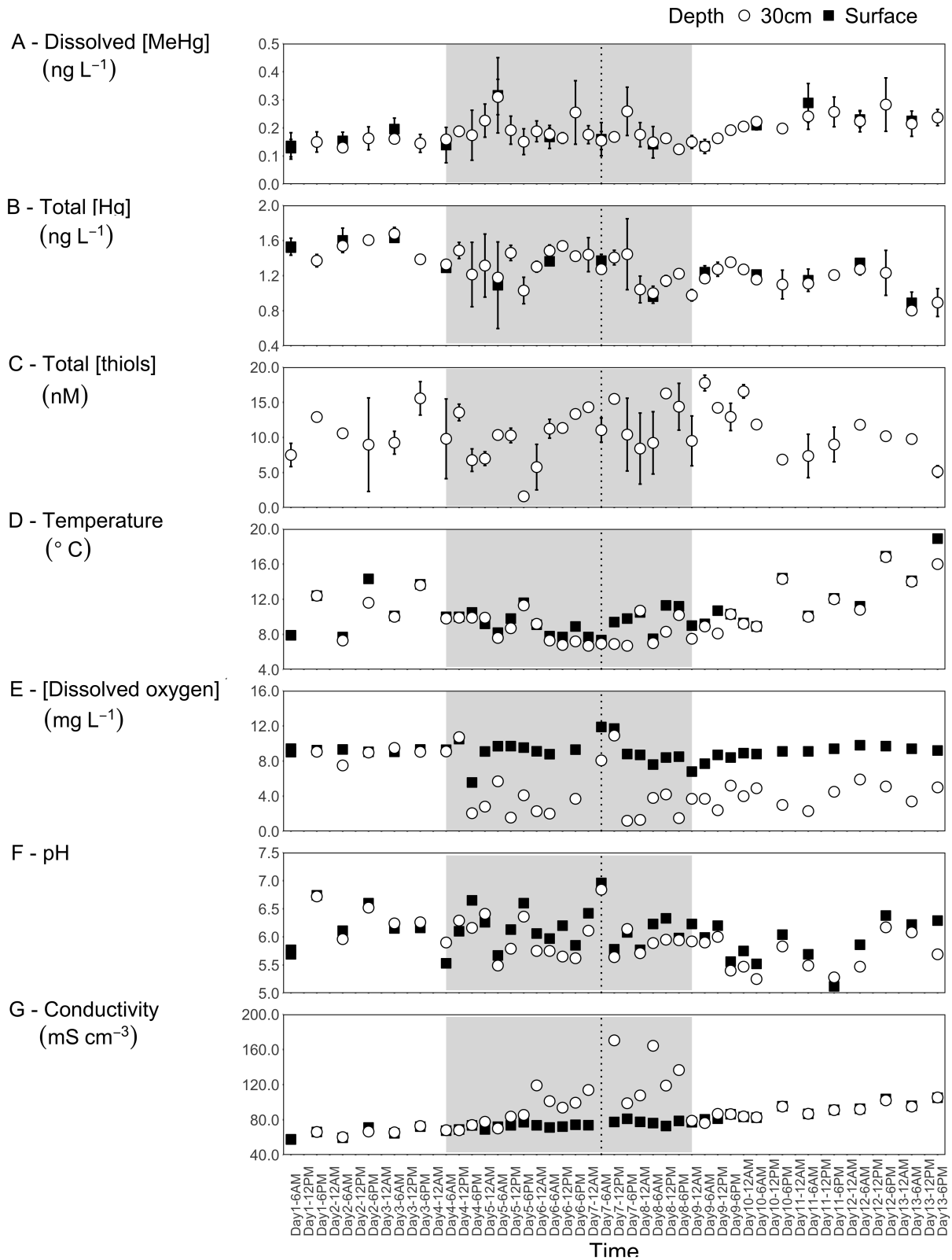
Depth ○ 30cm ■ Surface
A - Dissolved [MeHg] (ng L^{-1})
B - Total [Hg] (ng L^{-1})
C - Total [thiols] (nM)
D - Temperature (° C)
E - [Dissolved oxygen] (mg L^{-1})
F - pH
G - Conductivity (mS cm^{-3})
Time

Figure 5. Monitoring results of BYL22 during the covered pond experiment, at the surface and at a 30 cm depth. Grayed section represents the period during which the pond was covered. Dotted line represents momentarily exposed pond surface to light shortly after midnight on Day 7. **A.** MeHg concentrations (ng L^{-1}) over time. **B.** Total Hg concentrations (ng L^{-1}) over time. **C.** Total thiol concentrations (nM) over time (sum of glutathione, cysteine, thioglycolic acid, 3-mercaptopropionic acid, cysteine-glycine). **D.** Temperature (°C) over time. **E.** Dissolved oxygen (mg L^{-1}) over time. **F.** pH over time. **G.** Conductivity (μS cm^{-3}) over time.

ASSOCIATED CONTENT

Supporting Information. Details on physicochemical data tables for individual sites, raw incubation data, light attenuation by the tarpaulin and supplementary PD experiments. This material is available free of charge via the Internet at http://pubs.acs.org.

AUTHOR INFORMATION

Corresponding Author

* Marc Amyot. Phone: 514-343-7496. Fax: 514-343-2293. E-mail: m.amyot@umontreal.ca.Present Addresses

Author Contributions

The manuscript was written through contributions of all authors. All authors have given approval to the final version of the manuscript. CG and ML collected data. Data was analyzed by CG, ML and MA. All authors designed the experiments and prepared the manuscript.

Funding Sources

This research was funded through the Natural Sciences and Engineering Research Council (NSERC) Discovery grant to MA, the Northern Contaminants Program and the Northern Scientific Training Program (Aboriginal Affairs and Northern Development Canada). Student funding was provided by NSERC scholarships to CG.

Notes

The authors declare no competing financial interest.

ACKNOWLEDGMENT

The authors would like to thank Dominic Bélanger and Tania Sultana for support in the lab, as well as Isabelle Laurion, John Chételat, Alexandre Poulain, Brian Dimock and Pilipoosie Iqaluk for assistance in the field. This research was funded through the Natural Sciences and Engineering Research Council (NSERC) Discovery grant to MA, the Northern Contaminants Program and the Northern Scientific Training Program (Aboriginal Affairs and Northern Development Canada). Logistical support was provided by the Polar Continental Shelf Program (Natural Resources Canada), the Bylot Island Goose Camp (Université Laval) and Sirmilik National Park (Parks Canada). Student funding was provided by NSERC scholarships to CG.

REFERENCES

(1) Ariya, P. A.; Dastoor, A. P.; Amyot, M.; Schroeder, W. H.; Barrie, L.; Anlauf, K.; Raofie, F.; Ryzhkov, A.; Davignon, D.; Lalonde, J.; et al. The Arctic: a sink for mercury. *Tellus B* **2004**, *56*, 397–403.

(2) AMAP. *AMAP Assessment 2011: Mercury in the Arctic*; 2011.

(3) Compeau, G. C.; Bartha, R. Sulfate-reducing bacteria: principle methylators of mercury in anoxic estuarine sediment. *Appl. Environ. Microbiol.* **1985**, *50*, 498–502.

(4) Fleming, E. J.; Mack, E. E.; Green, P. G.; Nelson, D. C. Mercury methylation from unexpected sources: Molybdate-inhibited freshwater sediments and an iron-reducing bacterium. *Appl. Environ. Microbiol.* **2006**, *72*, 457–464.

(5) St Louis, V. L.; Sharp, M. J.; Steffen, A.; May, A.; Barker, J.; Kirk, J. L.; Kelly, D. J. A.; Arnott, S. E.; Keatley, B.; Smol, J. P. Some sources and sinks of monomethyl and inorganic mercury on Ellesmere Island in the Canadian High Arctic. *Enivronmental Sci. Technol.* **2005**, *39*, 2686–2701.

(6) Hamelin, S.; Amyot, M.; Barkay, T.; Wang, Y.; Planas, D. Methanogens : Principal Methylators of Mercury in Lake Periphyton. *Environ. Sci. Technol.* **2011**, *45*, 7693–7700.

(7) Hammerschmidt, C. R.; Fitzgerald, W. F. Photodecomposition of Methylmercury in an Arctic Alaskan Lake. *Environ. Sci. Technol.* **2006**, *40*, 1212–1216.

(8) Lehnherr, I.; St Louis, V. L.; Emmerton, C. A.; Barker, J. D.; Kirk, J. L. Methylmercury cycling in High Arctic wetland ponds: sources and sinks. *Environ. Sci. Technol.* **2012**, *46*, 10514–10522.

(9) Klaminder, J.; Yoo, K.; Rydberg, J.; Giesler, R. An explorative study of mercury export from a thawing palsa mire. *J. Geophys. Res.* **2008**, *113*, 1–9.

(10) Macdonald, R. W.; Harner, T.; Fyfe, J. Recent climate change in the Arctic and its impact on contaminant pathways and interpretation of temporal trend data. *Sci. Total Environ.* **2005**, *342*, 5–86.

(11) Rydberg, J.; Klaminder, J.; Rosén, P.; Bindler, R. Climate driven release of carbon and mercury from permafrost mires increases mercury loading to sub-arctic lakes. *Sci. Total Environ.* **2010**, *408*, 4778–4783.

(12) Stern, G. A.; Macdonald, R. W.; Outridge, P. M.; Wilson, S.; Chételat, J.; Cole, A.; Hintelmann, H.; Loseto, L. L.; Steffen, A.; Wang, F.; et al. How does climate change influence arctic mercury? *Sci. Total Environ.* **2012**, *414*, 22–42.

(13) Laird, B. D.; Shade, C.; Gantner, N.; Chan, H. M.; Siciliano, S. D. Bioaccessibility of mercury from traditional northern country foods measured using an in vitro gastrointestinal model is independent of mercury concentration. *Sci. Total Environ.* **2009**, *407*, 6003–6008.

(14) Pienitz, R.; Doran, P. T.; Lamoureux, S. Origin and geomorphology of lakes in the polar regions. In *Polar lakes and rivers: limnology of Arctic and Antarctic aquatic ecosystems*; Vincent, W. F.; Laybourn-Parry, J., Eds.; Oxford University Press: New York, 2008; p. 327.

(15) MacMillan, G. a.; Girard, C.; Chételat, J.; Laurion, I.; Amyot, M. High Methylmercury in Arctic and Subarctic Ponds is Related to Nutrient Levels in the Warming Eastern Canadian Arctic. *Environ. Sci. Technol.* **2015**, *49,* 7743–7753.

(16) Sellers, P.; Kelly, C. A.; Rudd, J. W. M.; MacHutchon, A. R. Photodegradation of methylmercury in lakes. *Nature* **1996**, *380*, 694–697.

(17) Li, Y.; Mao, Y.; Liu, G.; Tachiev, G.; Roelant, D.; Feng, X.; Cai, Y. Degradation of methylmercury and its effects on mercury distribution and cycling in the Florida Everglades. *Environ. Sci. Technol.* **2010**, *44*, 6661–6666.

(18) Zhang, T.; Hsu-Kim, H. Photolytic degradation of methylmercury enhanced by binding to natural organic ligands. *Nat. Geosci.* **2010**, *3*, 473–476.

(19) Lehnherr, I.; St Louis, V. L. Importance of ultraviolet radiation in the photodemethylation of methylmercury in freshwater ecosystems. *Environ. Sci. Technol.* **2009**, *43*, 5692–5698.

(20) Black, F. J.; Poulin, B. A.; Flegal, A. R. Factors controlling the abiotic photo-degradation of monomethylmercury in surface waters. *Geochim. Cosmochim. Acta* **2012**, *84*, 492–507.

(21) Suda, I.; Suda, M.; Hirayama, K. Degradation of methyl and ethyl mercury by singlet oxygen generated from sea water exposed to sunlight or ultraviolet light. *Arch. Toxicol.* **1993**, *67*, 365–368.

(22) Chen, J.; Pehkonen, S. O.; Lin, C. Degradation of monomethylmercury chloride by hydroxyl radicals in simulated natural waters. *Water Res.* **2003**, *37*, 2496–2504.

(23) Rose, C. H.; Ghosh, S.; Blum, J. D.; Bergquist, B. a. Effects of ultraviolet radiation on mercury isotope fractionation during photo-reduction for inorganic and organic mercury species. *Chem. Geol.* **2015**, *405*, 102–111.

(24) Sun, R.; Wang, D.; Zhang, Y.; Mao, W.; Zhang, T.; Ma, M.; Zhang, C. Photo-degradation of monomethylmercury in the presence of chloride ion. *Chemosphere* **2013**, *91*, 1471–1476.

(25) Sun, R.; Wang, D.; Mao, W.; Zhao, S.; Zhang, C.; Zhang, X. Photodegradation of methylmercury in the water body of the Three Gorges Reservoir. *Sci. China Chem.* **2015**, *58*, 1073–1081.

(26) Fernández-Gómez, C.; Drott, A.; Björn, E.; Diez, S.; Bayona, J. M.; Tesfalidet, S.; Lindfors, A.; Skyllberg, U. Towards universal wavelength specific photodegradation rate constants for methyl mercury in humic waters - exemplified by a boreal lake-wetland gradient. *Environ. Sci. Technol.* **2013**, *47*, 6279–6287.

(27) Hammerschmidt, C. R.; Fitzgerald, W. F. Iron-mediated photochemical decomposition of methylmercury in an Arctic Alaskan lake. *Environ. Sci. Technol.* **2010**, *44*, 6138–6143.

(28) Hintelmann, H.; Welbourn, P. M.; Evans, R. D. Measurement of complexation of methylmercury(II) compounds by freshwater humic substances using equilibrium dialysis. *Environ. Sci. Technol.* **1997**, *31*, 489–495.

(29) Fernández-Gómez, C.; Bayona, J. M.; Díez, S. Diffusive gradients in thin films for

predicting methylmercury bioavailability in freshwaters after photodegradation. *Chemosphere* **2015**, *131*, 184–191.

(30) Tai, C.; Li, Y.; Yin, Y.; Scinto, L. J.; Jiang, G.; Cai, Y. Methylmercury photodegradation in surface water of the Florida everglades: Importance of dissolved organic matter-methylmercury complexation. *Environ. Sci. Technol.* **2014**, *48*, 7333–7340.

(31) Chandan, P.; Ghosh, S.; Bergquist, B. A. Mercury Isotope Fractionation during Aqueous Photoreduction of Monomethylmercury in the Presence of Dissolved Organic Matter. *Environ. Sci. Technol.* **2014**, *49*, 259–267.

(32) Latch, D. E.; McNeill, K. Microheterogeneity of singlet oxygen distributions in irradiated humic acid solutions. *Science (80-.).* **2006**, *311*, 1743–1747.

(33) Qian, Y.; Yin, X.; Lin, H.; Rao, B.; Brooks, S. C.; Liang, L.; Gu, B. Why Dissolved Organic Matter Enhances Photodegradation of Methylmercury. *Environ. Sci. Technol. Lett.* **2014**, *1*, 426–431.

(34) Morris, D. P.; Zagarese, H.; Williamson, C. E.; Balseiro, E. G.; Hargreaves, B. R.; Modenutti, B.; Moeller, R.; Queimalinos, C. The attenuation of solar UV radiation in lakes and the role of dissolved organic carbon. *Limnol. Oceanogr.* **1995**, *40*, 1381–1391.

(35) Laurion, I.; Vincent, W. F.; Macintyre, S.; Retamal, L.; Dupont, C.; Francus, P.; Pienitz, R. Variability in greenhouse gas emissions from permafrost thaw ponds. *Limnol. Oceanogr.* **2010**, *55*, 115–133.

(36) Chételat, J.; Cloutier, L.; Amyot, M. Carbon sources for lake food webs in the Canadian High Arctic and other regions of Arctic North America. *Polar Biol.* **2010**, *33*, 1111–1123.

(37) St. Louis, V. L.; Rudd, J. W. M.; Kelly, C. A.; Beaty, K. G.; Bloom, N. S.; Flett, R. J. Importance of Wetlands as Sources of Methyl Mercury to Boreal Forest Ecosystems. *Can. J. Fish. Aquat. Sci.* **1994**, *51*, 1065–1076.

(38) Hu, H.; Mylon, S. E.; Benoit, G. Distribution of the thiols glutathione and 3-mercaptopropionic acid in Connecticut lakes. *Limnol. Oceanogr.* **2006**, *51*, 2763–2774.

(39) Labonté-David, E. Relation entre les espèces de mercure, le sélénium et les thiols dans les eaux de surface du parc national du Mont-Tremblant (Laurentides, Québec), Université de Montréal, 2012.

(40) Leclerc, M.; Planas, D.; Amyot, M. Relationship Between Extracellular Low Molecular Weight Thiols and Mercury Species in Natural Lake Periphytic Biofilms. *Environ. Sci. Technol.* **2015**, *49*, 7709–7716.

(41) Zhang, J. Z.; Wang, F. Y.; House, J. D.; Page, B. Thiols in wetland interstitial waters and their role in mercury and methylmercury speciation. *Limnol. Oceanogr.* **2004**, *49*, 2276–2286.

(42) Liem-Nguyen, V.; Bouchet, S.; Björn, E. Determination of sub-nanomolar levels of low molecular mass thiols in natural waters by liquid chromatography tandem mass spectrometry after derivatization with p-(hydroxymercuri) benzoate and online preconcentration. *Anal. Chem.* **2015**, *87*, 1089–1096.

(43) Arp, C. D.; Jones, B. M.; Schmutz, J. a.; Urban, F. E.; Jorgenson, M. T. Two mechanisms of aquatic and terrestrial habitat change along an Alaskan Arctic coastline. *Polar Biol.* **2010**, *33*, 1629–1640.

(44) Perron, T.; Chételat, J.; Gunn, J.; Beisner, B. E.; Amyot, M. Effects of Experimental Thermocline and Oxycline Deepening on Methylmercury Bioaccumulation in a Canadian Shield Lake. *Environ. Sci. Technol.* **2014**, *48*, 2626–2634.

(45) Amyot, M.; Lean, D.; Mierle, G. Photochemical formation of volatile mercury in high Arctic lakes. *Environ. Toxicol. Chem.* **1997**, *16*, 2054–2063.

(46) Tipping, E.; Lofts, S.; Sonke, J. E. Humic Ion-Binding Model VII: a revised parameterisation of cation-binding by humic substances. *Environ. Chem.* **2011**, *8*, 225–235.

(47) R Core Team. R: A language and environment for statistical computing. *R Foundation for Statistical Computing*, 2015.

(48) Garcia, E.; Amyot, M.; Ariya, P. Relationship between DOC photochemistry and mercury redox transformations in temperate lakes and wetlands. *Geochim. Cosmochim. Acta* **2005**, *69*, 1917–1924.

(49) Ravichandran, M. Interactions between mercury and dissolved organic matter - a review. *Chemosphere* **2004**, *55*, 319–331.

(50) Waples, J. S.; Nagy, K. L.; Aiken, G. R.; Ryan, J. N. Dissolution of cinnabar (HgS) in the presence of natural organic matter. *Geochim. Cosmochim. Acta* **2005**, *69*, 1575–1588.

(51) Jeremiason, J.; Portner, J. C.; Aiken, G.; Tran, K. T.; Dvorak, M. T.; Hiranaka, A.; Latch, D. Photoreduction of Hg(II) and photodemethylation of methylmercury: The key role of thiol sites on dissolved organic matter. *Environ. Sci. Process. Impacts* **2015**, *17*, 1892–1903.

(52) Moingt, M.; Bressac, M.; Bélanger, D.; Amyot, M. Role of ultra-violet radiation, mercury and copper on the stability of dissolved glutathione in natural and artificial freshwater and saltwater. *Chemosphere* **2010**, *80*, 1314–1320.

(53) Zepp, R. G. Photochemical conversion of solar energy in the environment. In *Photochemical conversion and storage of solar energy*; Pelizzetti, E.; Schiavello, M., Eds.; Kluwer Academic Publishers: Dordrecht, Netherlands, 1991; pp. 497–515.

(54) Kieber, D. J.; Peake, B. M.; Scully, N. M. Reactive oxygen species in aquatic ecosystems. In *UV effects in aquatic organisms and ecosystems*; Helbling, E. W.; Zagarese, H., Eds.; The Royal Society of Chemistry: Cambridge, United Kingdom, 2003; pp. 251–288.

(55) Scully, N. M.; Lean, D. R. S.; Mcqueen, D. J.; Cooper, W. Photochemical formation of hydrogen peroxide in lakes : effects of dissolved organic carbon and ultraviolet radiation. *Can. J. Fish. Aquat. Sci.* **1995**, *52*, 2675–2681.

(56) French, T. D.; Houben, A. J.; Desforges, J.-P. W.; Kimpe, L. E.; Kokelj, S. V; Poulain, A. J.; Smol, J. P.; Wang, X.; Blais, J. M. Dissolved Organic Carbon Thresholds Affect Mercury Bioaccumulation in Arctic Lakes. *Environ. Sci. Technol.* **2014**, *48*, 3162–3168.

(57) Driscoll, C. T.; Yan, C.; Schofield, C. L.; Munson, R.; Holsapple, J. The mercury cycle and fish in the Adirondack lakes. *Environ. Sci. Technol.* **1994**, *28*, 136A – 143A.

(58) Sobek, S.; Tranvik, L. J.; Prairie, Y. T.; Kortelainen, P.; Cole, J. J. Patterns and regulation of dissolved organic carbon: An analysis of 7,500 widely distributed lakes. *Limnol. Oceanogr.* **2007**, *52*, 1208–1219.

(59) Smith, L. C.; Sheng, Y.; MacDonald, G. M. A First Pan-Arctic Assessment of the Influence of Glaciation, Permafrost,Topography and Peatlands on Northern Hemisphere Lake Distribution. *Permafr. Periglac. Process.* **2007**, *18*, 201–208.

(60) Whalin, L.; Kim, E.; Mason, R. Factors influencing the oxidation, reduction, methylation and demethylation of mercury species in coastal waters. *Mar. Chem.* **2007**, *107*, 278–294.

(61) Kim, M.-K.; Won, A.-Y.; Zoh, K.-D. The production of dissolved gaseous mercury from methylmercury photodegradation at different salinity. *Desalin. Water Treat.* **2016**, *57*, 610–619.

(62) Grégoire, D. S.; Poulain, A. J. A little bit of light goes a long way: the role of phototrophs on mercury cycling. *Metallomics* **2014**, *6*, 396–407.

(63) Sellers, P.; Kelly, C. A.; Rudd, J. W. M. Fluxes of methylmercury to the water column of a drainage lake: The relative importance of internal and external sources. *Limnol. Oceanogr.* **2001**, *46*, 623–631.

(64) Hammerschmidt, C. R.; Fitzgerald, W. F. Formation of artifact methylmercury during extraction from a sediment reference material. *Anal. Chem.* **2001**, *73*, 5930–5936.

(65) Pak, K.; Bartha, R. Mercury Methylation and Demethylation in Anoxic Lake Sediments and by Strictly Anaerobic Bacteria Mercury Methylation and Demethylation in Anoxic Lake Sediments and by Strictly Anaerobic Bacteria. *Appl. Environ. Microbiol.* **1998**, *64*, 1013–1017.

(66) Bergquist, B. a; Blum, J. D. Mass-dependent and -independent fractionation of hg isotopes by photoreduction in aquatic systems. *Science* **2007**, *318*, 417–420.

TOC/ABSTRACT ART : Methylmercury is photodemethylated in Arctic thaw ponds.

Supplementary information

Photodemethylation of methylmercury in Eastern Canadian Arctic thaw pond and lake ecosystems

*Catherine Girard[1], Maxime Leclerc[2], Marc Amyot[1,2]**

AUTHOR ADDRESS

1. Centre d'études nordiques (CEN), Département de sciences biologiques, Université de Montréal, 90 Vincent-d'Indy, Montréal, QC, Canada

2. Groupe de recherche interuniversitaire en limnologie et en environnement aquatique (GRIL) , Département de sciences biologiques, Université de Montréal, 90 Vincent-d'Indy, Montréal, QC, Canada

*Corresponding author:

Marc Amyot. Phone: 514-343-7496. Fax: 514-343-2293. E-mail: m.amyot@umontreal.ca.

Supporting information consists of 16 pages with 4 tables and 7 figures.

TABLE OF CONTENTS

Supplementary methods

Certified standard solutions

MeHg solution used for 5.0 ng L^{-1} amendments was made from a MeHg stock solution (1000 ppm, certified by Alfa Aesar). A 1 ppm MeHg solution was prepared by dilution in methanol (Fisher Scientific, HPLC grade). Intermediate and working solutions (10.0 ug L^{-1}, 600 ng L^{-1} and 10 ng L^{-1}) were prepared in MilliQ water (18.2 MΩ cm, EMD Millipore) and preserved with 0.3% acetic acid (Fisher Scientific, ACS-pur) and 0.2% HCL (EMD, Omni-trace ultra).

Sampling methods

Sampling and experimental solution bottles were rinsed with distilled water, then soaked in a 45% HNO_3, 5% HCl (Fisher Scientific, ACS-pur) bath overnight, before being rinsed 3 times with MilliQ water (18.2 MΩ cm, EMD Millipore).

The peristaltic pump used for sampling was flushed with a 10% HCl solution (Fisher Scientific, ACS-pur) for 10 minutes, then rinsed with site water for 10 minutes.

Vertical profiles in the water column for water conductivity, pH, temperature and dissolved oxygen were measured using a YSI 650 data logger (YSI Incorporated/Xylem Incorporated). Solar radiation data was collected during experiments with Hobo photosynthetic light (PAR) sensors and data loggers (Onset), and light measurements were collected with a Jaz spectrometer (Ocean Optics). Light attenuation coefficients at each study site were calculated with the Beer-Lambert law:

$$I_z = I_0 e^{-kz} \quad \text{(S1)}$$

where z is a given depth in the water column (m), I_z is the intensity of light (W m^{-2}) measured at depth z (Jaz; 290-895 nm), I_o is the intensity of light at the surface (W m^{-2}) and k is the light attenuation coefficient.

Analytical methods

DOC levels were quantified with an Aurora 1030 analyzer (OI Analytical) by persulfate heat oxidation, followed by conductiometric determination of released CO_2. Anions were analyzed via ionic chromatography (Waters), while cations were measured with flame atomic absorption spectroscopy (Varian, Agilent). Total (reduced and oxidized species) thiols (glutathione, cysteine, thioglycolic acid, 3-mercaptopropionic acid, cysteine-glycine) were analyzed by derivatization using ammonium 7-fluorobenzo-2-oxa-1,3-diazole-sulfonate (SBD-F) (Fluka Analytical, Sigma-Aldrich) and high performance liquid chromatography with a fluorescence detector, as described in Moingt et al.[1] Thiol detection limit was defined as three times the standard deviation calculated on 10 low concentration (< 5 nM) standards. These were 1.0 nM for glutathione, 1.0 nM for cysteine, 1.1 nM for thioglycolic, 2.2 nM for 3-mercaptopropionic acid, and 0.4 nM for cysteine-glycine.

Experimental design

Photodemethylation field experiments were conducted in natural sunlight. Water was collected in clear, acid-washed Teflon bottles with no headspace. On Bylot, bottles were incubated in floating rafts approximately 0.5 cm below the surface of the sampled pond. On Cornwallis, due to weather, incubations were conducted in basins on the shore, in water changed periodically to prevent warming. In all cases, bottles were placed horizontally with their caps pointing north to

insure uniform irradiation.[2] At every time-point, a triplicate of every treatment series (or duplicate for dark controls) was removed from the incubation set-up and preserved with ultrapure HCl to a 0.4% final concentration. The bottles were then stored in the dark at 4 °C until analysis.

In experiments measuring natural rates conducted in BYL24 and Char Lake, water was collected and separated into three treatment series: one control series kept in the dark, a series exposed to the full spectrum of sunlight and a series exposed to the visible spectrum only using UV filters (transmission of approximately 16% for wavelengths (λ) <400 nm, and 100% for 400 $\leq \lambda \leq$ 700 nm) (Lee 226, Lee Filters).

Mechanistic experiments aiming to study the effect of chemical actors on photodemethylation were also conducted in the field at BYL22 and Char Lake. All bottles were spiked with 5.0 ng L^{-1} (± 0.4%) of MeHg, and treatments included thiols (10 nM glutathione (*GSH*), 10 nM thioglycolic acid (*TA*)) (formation constants for complexation to MeHg at pH 7.4: *GSH* = 11.55, *TA* = 11.47)[3,4] and chlorides (0.6 M of Cl). Incubations lasted 50 h. This experiment was repeated in the laboratory in a Suntest CPS+ solar simulator (Atlas Material Testing Technology) using BYL22 and MilliQ water. To insure comparability between field experiments and data generated in the laboratory, Hobo photosynthetically active radiation (*PAR*) sensors (Onset) were used to collect light measurements in the field, which were compiled to establish a total irradiance dose received during field experiments. The Suntest CPS+ (Atlas Material Testing Technology) was programmed to deliver constant total irradiance during artificial incubations, with a total dose equal to that received during field incubations but over a shorter period. This required using higher intensity irradiation than what naturally occurred on the field, with a lamp producing a slightly different wavelength spectrum (notably more UV-A radiation than sunlight on the field,

and the absence of UV-C radiation) (SI Table S4). No replicates were done in this experiment, due to limited space in the solar simulator.

Finally, to assess the potential impact of photodemethylation on the MeHg budget of an aquatic ecosystem, we sampled BYL22 every 6 h (surface and 30 cm depth) over a 14-day period for total Hg and MeHg and water chemistry parameters. During days 4-8, the pond was covered with a clean opaque plastic tarpaulin anchored into the surrounding permafrost. Pump and sensor tubing were permanently installed at the desired depths to limit disturbances and light penetration associated with sampling. Water was pumped continuously during 5 minutes before each sampling, to thoroughly rinse system.

Supplementary results & discussion

Predicted MeHg losses in covered pond experiment

Theoretical MeHg losses following re-exposure of pond surface to sunlight were calculated using equation 1. This accounts for predicted photodemethylation occurring during Days 9-13, using BYL22 k_{PD} (9.3×10^{-3} m^2 E^{-1}), average daily *PAR* on Bylot Island (37.76 E d^{-1}) (SI, Table S1) and MeHg concentration on Day 9 (1.35 ng L^{-1}) (Figure 5).

$$\ln([MeHg]_t) = \ln([MeHg]_0) - k_{PD}PAR_t \quad (1)$$

$$\ln([MeHg]_{Day13}) = \ln([MeHg]_{Day9}) - k_{PD}PAR_t$$

$$\ln([MeHg]_{Day13}) = \ln(0.14 \text{ ng } L^{-1}) - (9.3 \times 10^{-3} \text{ m}^2 \text{ E}^{-1}) \times (37.76 \text{ E m}^{-2} \text{ d}^{-1} \times 5 \text{ days})$$

$$\ln([MeHg]_{Day13}) = -1.97 - 1.76$$

$$\ln([MeHg]_{Day13}) = -3.73$$

$MeHg_{Day13} = 0.02$ ng L^{-1}

Predicted % of MeHg loss = $1 - MeHg_{Day13}/MeHg_{Day9} \times 100$

Predicted % of MeHg loss = $1 - 0.02$ ng $L^{-1}/0.14$ ng $L^{-1} \times 100$

Predicted % of MeHg loss = 85.71%

Note that this loss is only applicable to the surface and should be compared to the surface data in Fig. 5. We only considered the surface here, and assumed that the water was not mixing well after the removal of the cover. This assumption is based on the oxygen data in Fig. 5 that indicated an oxygen stratification from Day 4 to Day 13. We consider the 85% loss as an upper limit.

Supplementary references

(1) Moingt, M.; Bressac, M.; Bélanger, D.; Amyot, M. Role of ultra-violet radiation, mercury and copper on the stability of dissolved glutathione in natural and artificial freshwater and saltwater. *Chemosphere* **2010**, *80*, 1314–1320.

(2) Poulain, A. J.; Lalonde, J. D.; Amyot, M.; Shead, J. A.; Raofie, F.; Ariya, P. A. Redox transformations of mercury in an Arctic snowpack at springtime. *Atmos. Environ.* **2004**, *38*, 6763–6774.

(3) Reid, R. S.; Rabenstein, D. L. Nuclear Magnetic Resonance Studies of the Solution Chemistry of Metal Complexes . 19 . Formation Constants for the Complexation of Methylmercury by Glutathione , Ergothioneine , and Hemoglobin. *J. Am. Chem. Soc.* **1982**, *104*, 6733–6737.

(4) Reid, R. S.; Rabenstein, D. L. Nuclear magnetic resonance studies of the solution chemistry of metal complexes . XVII . Formation constants for the complexation of methylmercury by sulfhydryl- containing amino acids and related molecules. *Can. J. Chem.* **1981**, *59*, 1505–1514.

(5) CEN 2014. *Données environnementales de l'île Bylot au Nunavut, Canada, v 1.4 (1992-2014)*.

(6) Weather Canada. Historical Climate Data http://climate.weather.gc.ca/index_e.html#access.

(7) Black, F. J.; Poulin, B. A.; Flegal, A. R. Factors controlling the abiotic photo-degradation

of monomethylmercury in surface waters. *Geochim. Cosmochim. Acta* **2012**, *84*, 492–507.

(8) Fernández-Gómez, C.; Drott, A.; Björn, E.; Diez, S.; Bayona, J. M.; Tesfalidet, S.; Lindfors, A.; Skyllberg, U. Towards universal wavelength specific photodegradation rate constants for methyl mercury in humic waters - exemplified by a boreal lake-wetland gradient. *Environ. Sci. Technol.* **2013**, *47*, 6279–6287.

(9) Lehnherr, I.; St Louis, V. L. Importance of ultraviolet radiation in the photodemethylation of methylmercury in freshwater ecosystems. *Environ. Sci. Technol.* **2009**, *43*, 5692–5698.

(10) Lehnherr, I.; St Louis, V. L.; Emmerton, C. A.; Barker, J. D.; Kirk, J. L. Methylmercury cycling in High Arctic wetland ponds: sources and sinks. *Environ. Sci. Technol.* **2012**, *46*, 10514–10522.

(11) Hammerschmidt, C. R.; Fitzgerald, W. F. Photodecomposition of Methylmercury in an Arctic Alaskan Lake. *Environ. Sci. Technol.* **2006**, *40*, 1212–1216.

(12) Perron, T.; Chételat, J.; Gunn, J.; Beisner, B. E.; Amyot, M. Effects of Experimental Thermocline and Oxycline Deepening on Methylmercury Bioaccumulation in a Canadian Shield Lake. *Environ. Sci. Technol.* **2014**, *48*, 2626–2634.

Supplementary tables

Table S1. Surface water chemistry and Hg values measured at each site in 2010, where *Lat*. is latitude, *Long*. is longitude, *Temp*. is water temperature, *Cond*. Is conductivity, *DO* is dissolved oxygen z_{max} is maximum depth, *k* is light attenuation coefficient, *PAR* is photosynthetically active radiation measured during field experiments, air *temp*. is temperature during field experiments on Bylot[5] and Cornwallis[6] Islands and *DOC* is dissolved organic carbon.

Site		*Lat*. (°N)	*Long*. (°W)	Type	*Temp*. (°C)	*Cond*. (µS cm^{-1})	*DO* (mg L^{-1})	pH	z_{max} (m)	*k*	Average daily *PAR* (E d^{-1})	Average air *temp*. (°C)
Bylot Island	BYL22	73°9'29"	-79°58'44"	Pond	15.37	38	25.90	7.24	1.00	3.42	37.76 ± 16.13	5.71 ± 1.11
	BYL24	73°9'26"	-79°58'42"	Pond	10.5	50	12.09	7.22	0.39	1.37		
Cornwallis Island	Char	74°42'16"	-94°52'56"	Lake	5.59	264	10.60	7.92	27.50	0.84	24.62 ± 13.04	4.93 ± 1.70

(Table S1 continued)

Site		[Hg_{tot}] (ng L^{-1})	[MeHg] (ng L^{-1})	*DOC* (mg L^{-1})	Cl (mg L^{-1})	NO_3 (mg L^{-1})	NO_2 (mg L^{-1})	SO_4 (mg L^{-1})	F (mg L^{-1})	Ca (mg L^{-1})	Mg (mg L^{-1})	Na (mg L^{-1})	K (mg L^{-1})
Bylot Island	BYL22	2.38 ± 0.02	0.35 ± 0.04	6.20	2.88	0.12	<0.004	1.81	0.12	-	-	-	-
	BYL24	2.97 ± 0.06	0.70 ± 0.05	9.60	3.99	0.09	<0.004	1.62	0.14	-	-	-	-
Cornwallis Island	Char	0.44 ± 0.11	0.02 ± 0.004	0.94	21.54	<0.62	-	26.35	-	33.59	5.30	10.76	1.07

Table S2. Comparison of photodemethylation first-order rates (k_{PD}) measured in recent studies against photosynthetically active radiation (PAR). Surface measurements in natural freshwater only. *Average over 3 years.

Study	Site	k_{PD} (m^2 E^{-1}) $\times 10^{-3}$ from PAR	*DOC* (mg L^{-1})	pH
Present study	Thaw ponds on Bylot Island, Nunavut	6.0 – 9.2	0.94 – 9.60	7.22 – 7.92
Black et al., 2012[7]	Coastal wetlands near San Francisco, California	9.9 ± 2.0 (6.0 – 15.0)	6	6.50
Fernandez-Gomez et al., 2013[8]	Boreal lakes north of Umeå, Sweden	2.3 ± 0.2	17.50 – 81.00	3.80 – 6.60
Lehnherr and St-Louis, 2009[9]	Lake 979 at the Experiment Lakes Area, Ontario	4.4	12.80	N/A
Lehnherr et al., 2012[10]	Wetland ponds near Lake Hazen, Nunavut	3.2 – 3.6	5.73 – 10.87*	8.50 – 8.75
Hammerschmidt and Fitzgerald, 2006[11]	Toolik Lake, Alaska	2.6	4.40	7.60

Table S3. All rates obtained in this study. k_{PDs} (m^2 E^{-1}) are presented with standard error, R^2 adjusted and slope *p*-value. For significant slopes, Bonferroni-corrected ANCOVA results are presented to identify in-experiment differences between slopes. **Figure 1.** Experiment conducted on the field in BYL24, with exposure to full spectrum and *PAR* only. **Figure 2.** Experiment conducted on the field in BYL22. Water samples were amended to 5 ng L^{-1} of MeHg and exposed to full spectrum light. **Figure 3.** Experiment conducted on the field in BYL22 and Char Lake, and solar simulator incubations using BYL22 and MilliQ water. Water samples were amended to 5 ng L^{-1} and treated with *GSH*, *TA* or Cl.

Site	Treatment	$k_{PD} \times 10^{-3}$ m^2 E^{-1}	St.err x 10^{-3} m^2 E^{-1}	R^2 adjusted	k_{PD} *p*-value	ANCOVA
Figure 1 – k_{PDs} at ambient MeHg concentrations in natural waters						
BYL24	Dark control	0.6	0.9	-17.6%	Not significant	-
	Full spectrum	-6.1	0.7	95.5%	< 0.005**	a
	PAR only	0.0	1.0	-33.3%	Not significant	-
Figure 2 – k_{PDs} in spiked natural waters						
A - BYL22	Dark control	-0.9	-	-	-	-
	Full spectrum	-9.3	1.5	82.1%	< 0.0005***	a
Inset (first 12h)	Full spectrum	-3.1	5.3	-14.8%	Not significant	-
B – Char Lake	Dark control	-2.2	-	-	-	-
	Full spectrum	-3.2	1.7	24.6%	Not significant	-
Inset (first 12h)	Full spectrum	-19.3	5.9	66.0%	< 0.05*	a
Figure 3 – k_{PDs} in spiked natural waters according to treatment in the field or in a solar simulator						
A - BYL22	Control	-9.3	1.5	82.1%	< 0.0005***	a
	Cl	-6.7	0.6	93.5%	< 0.00005***	a
	TA	-6.2	1.0	82.1%	< 0.0005***	a
B - Char Lake	Control	-3.2	1.7	24.6%	Not significant	-
	GSH	-0.6	0.7	-4.3%	Not significant	-
	Cl	-3.3	1.6	28.9%	Not significant	-
	TA	0.2	1.0	-13.9%	Not significant	-
Inset (first 12h)	Control	-19.3	5.9	66.0%	< 0.05*	a
	GSH	-19.3	4.0	82.1%	< 0.01**	a
	Cl	-16.3	6.8	48.7%	Not significant	-
	TA	-15.2	7.2	40.8%	Not significant	-
C - BYL22 in solar simulator	Control	-11.3	2.4	84.0%	< 0.05*	a
	GSH	-11.0	0.8	97.7%	< 0.001***	a
D – MilliQ in solar simulator	Dark control	0.8	2.4	-28.4%	Not significant	-
	Control	-6.1	0.5	97.3%	< 0.005**	a
	GSH	-8.0	2.7	65.8%	Not significant	-

Table S4. Comparison on UV spectrum delivered by Suntest CPS+ and sunlight on Bylot Island during experiments.

UV radiation	Irradiance (photons cm^{-2} s^{-1})	
	Suntest CPS+	Bylot Island sunlight
Total UVs (100 – 400 nm)	5.69×10^{15}	2.16×10^{15}
UV-A (320 – 400 nm)	5.61×10^{15}	2.08×10^{15}
UV-B (290 – 320 nm)	9.36×10^{13}	6.44×10^{13}

Supplementary figures

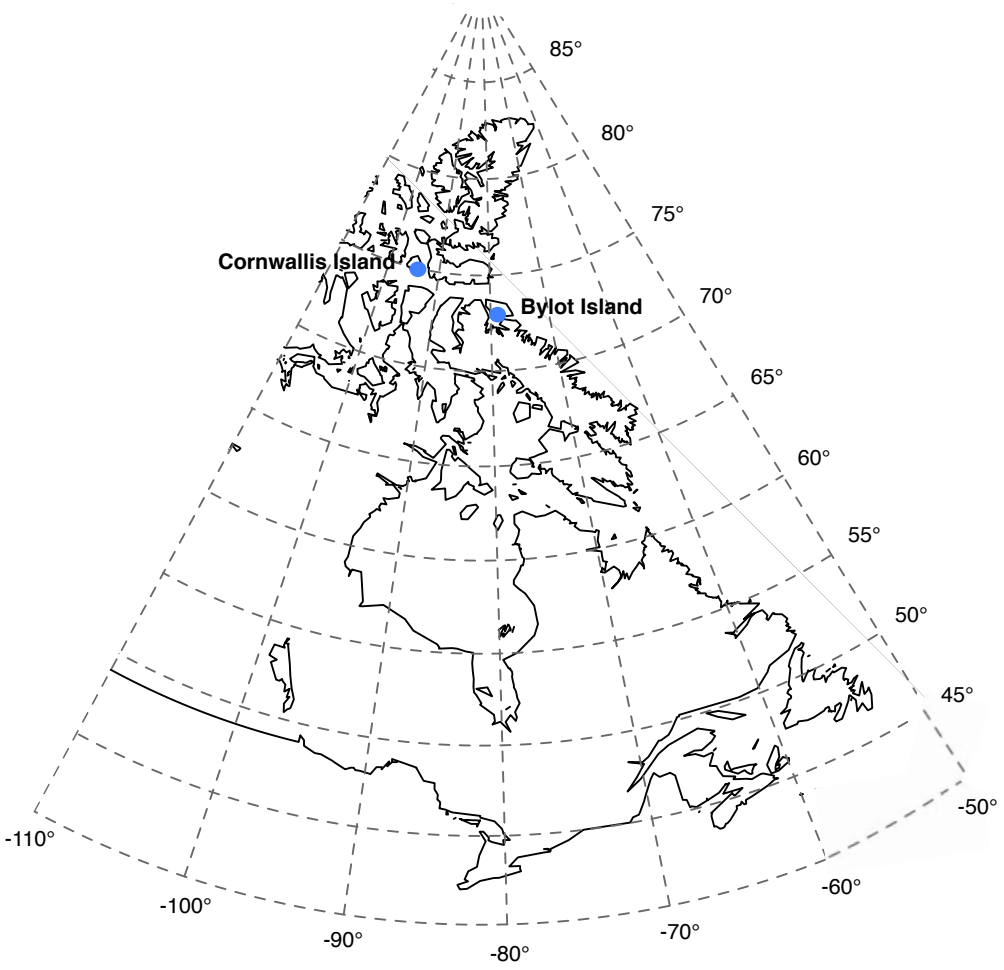

Figure S1. Map of Cornallis and Bylot Islands in the Canadian Arctic Archipelago.

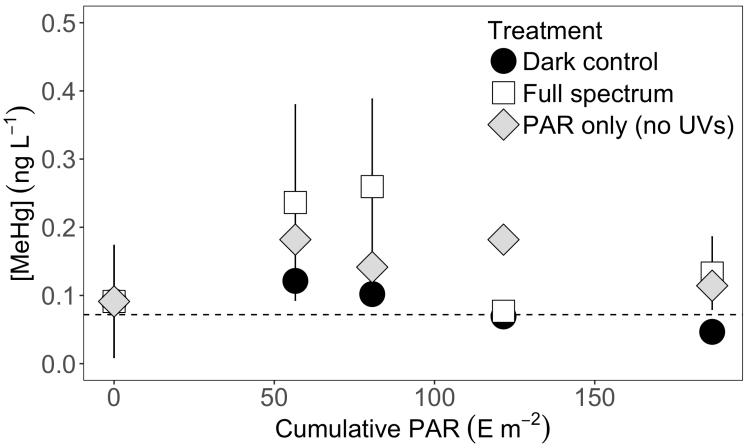

Figure S2. Raw MeHg data for experiment conducted in Char Lake. Some data points were below field detection limit, represented by the dotted line (3x standard deviation of triplicate control = 0.07 ng L^{-1}).

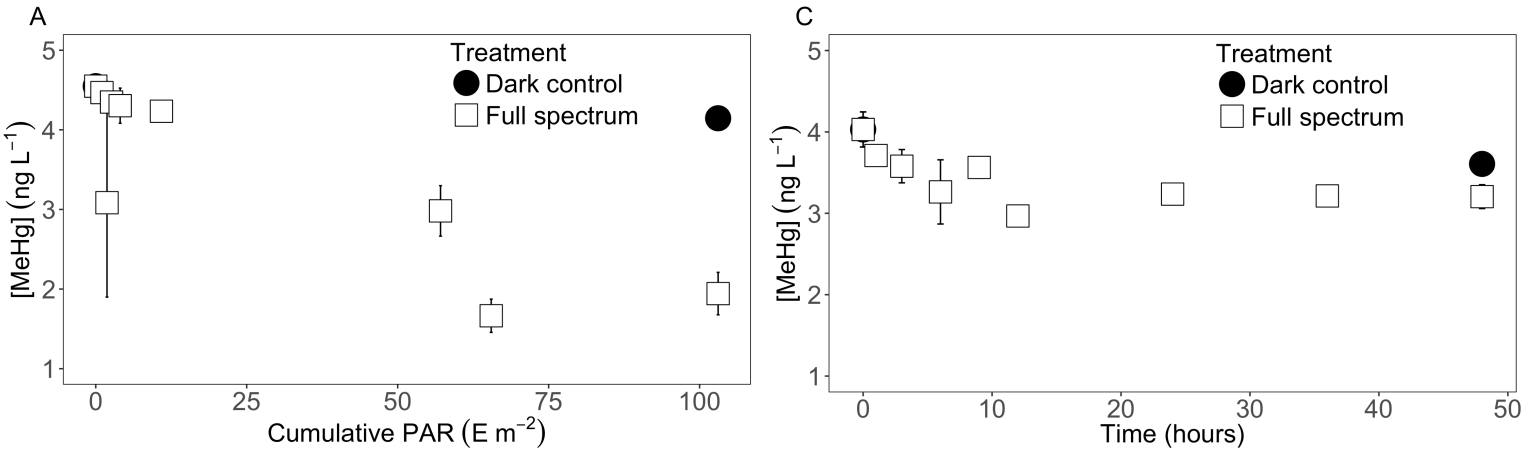

Figure S3. Raw MeHg data for experiment conducted in BYL22 and Char Lake, presented in Figure 2.

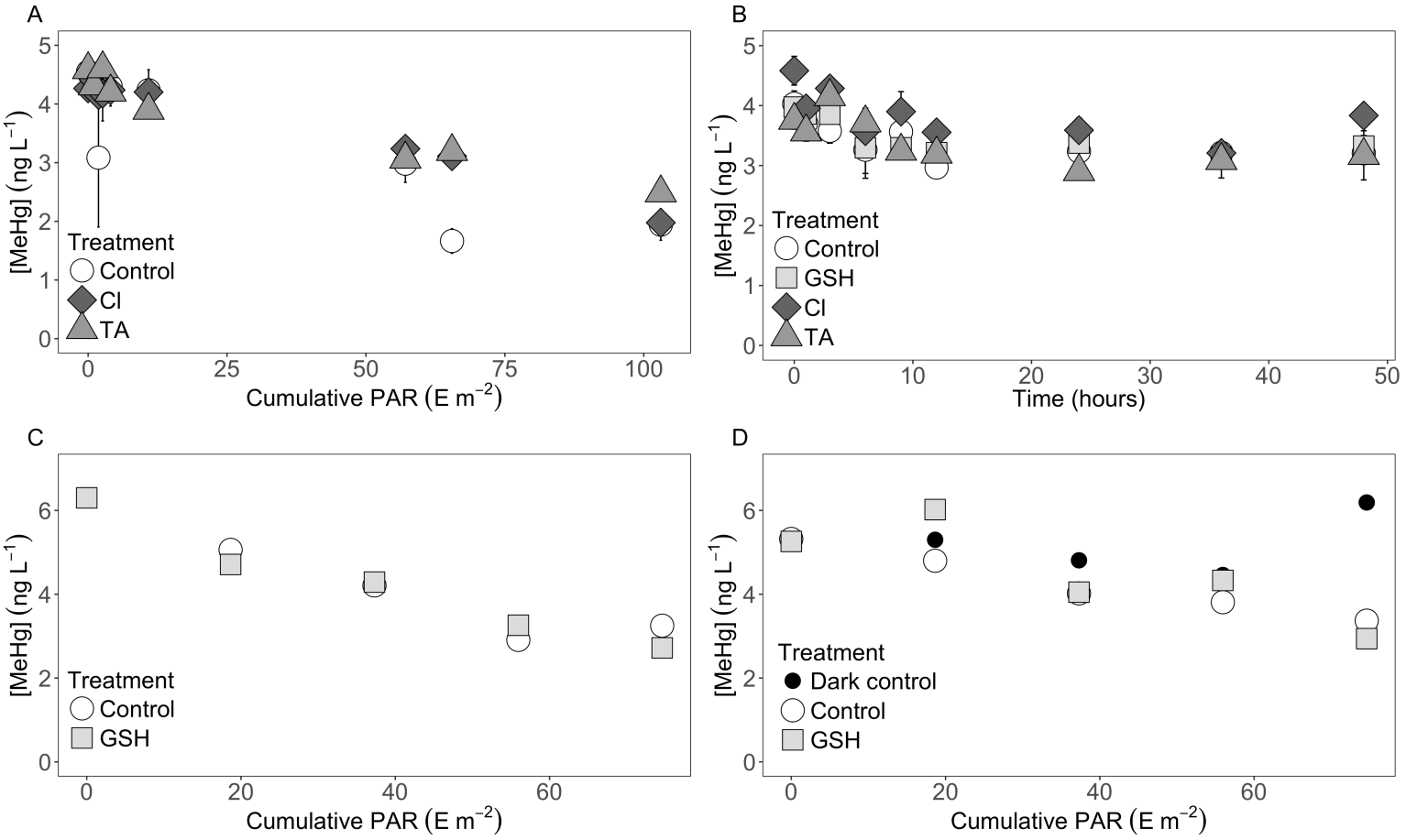

Figure S4. Raw MeHg data for experiment conducted on the field (BYL22 and Char Lake) and in the simulator with (MilliQ and BYL22 water), presented in Figure 3C and 3D.

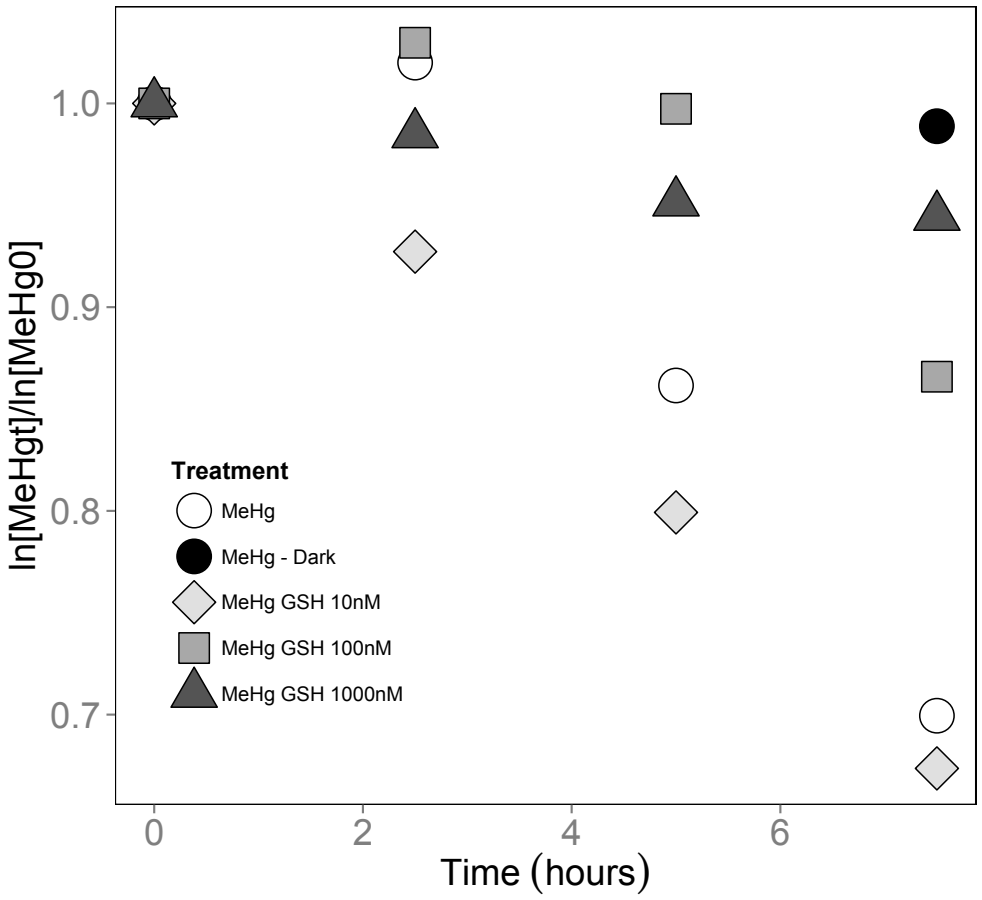

Figure S5. Photodemethylation experiment conducted in a solar simulator using water from a temperate lake (Lake Croche, described in Perron et al.[12]), in the presence of varying concentrations of *GSH* (10-1000 nM) over time (hours).

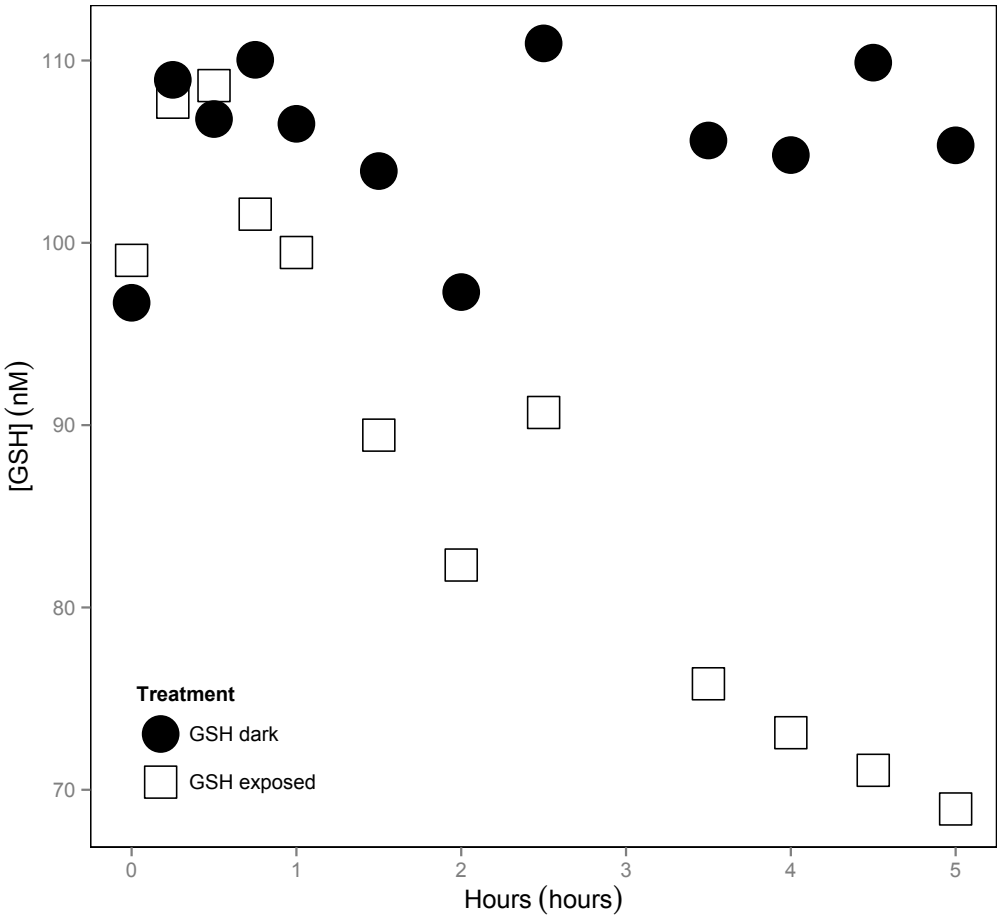

Figure S6. Degradation of *GSH* over time during irradiation in a solar simulator using water from a temperate lake (Lake Croche, described in Perron et al.[12]).

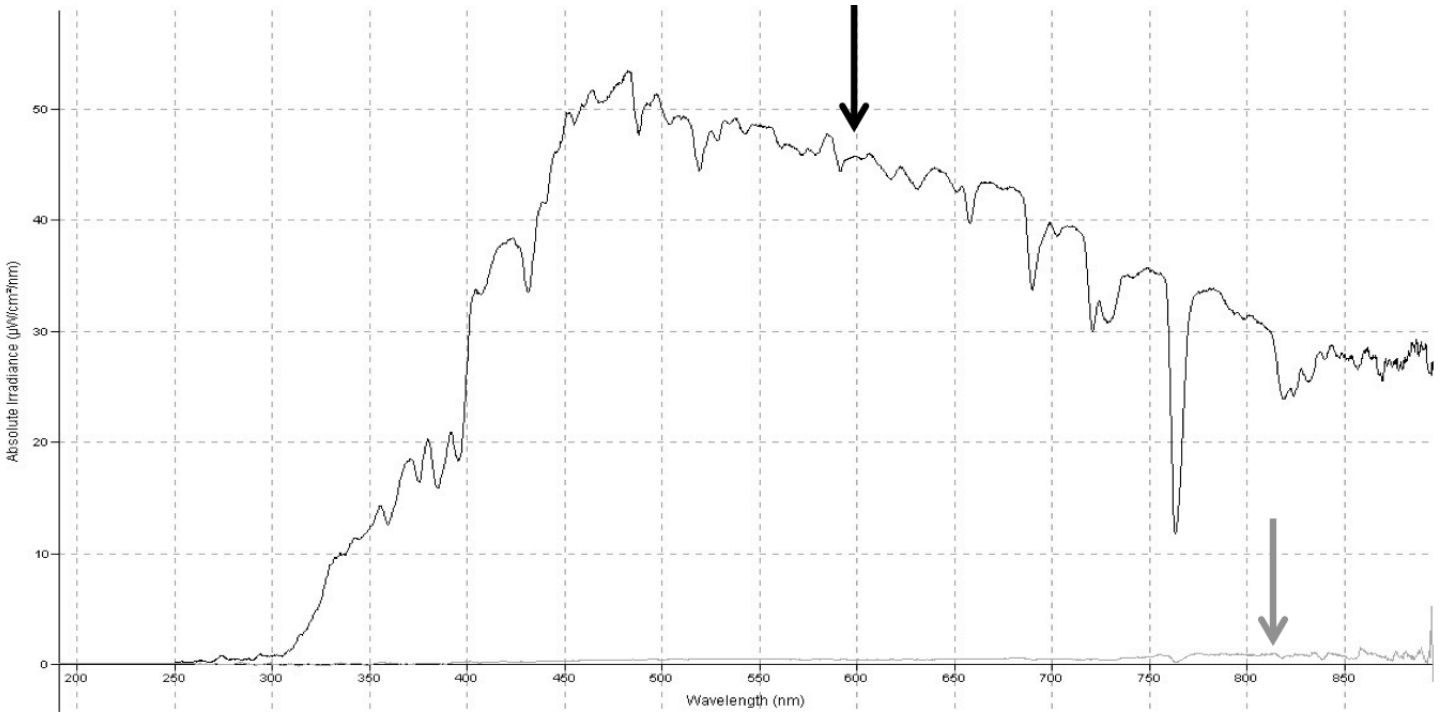

Figure S7. Absolute irradiance (µW cm^{-2} nm^{-1}) spectrum above (in black) and under (in gray) the plastic tarpaulin used in the covered pond experiment, showing radiation obstruction of 98.7% of radiation from 290-895 nm, and 100% of radiation in the UV spectrum (400 nm ≤ λ